Semester project

XBAR resonators in 128° Y-cut Lithium Niobate LiNbO3

Author
Manal Zeddoug

Professor
Guillermo Villanueva
Supervisor
Soumya Yandrapalli

June 10, 2021

Contents

1 Introduction

The increasing demand of higher frequencies technologies in RF (Radio frequency) components, especially for telecommunication, create a need to develop wider and higher frequency bands filters, with optimal performances. Thus, constant effort are made to develop new resonators that outperform excited technologies mainly in terms of electromechanical coupling and quality factor.

EXcited Bulk Acoustic Resonator XBAR which are composed of a single piezoelectric crystal layer, with metallic electrodes on the top surface, seem to be an interesting solutions. It has indeed been shown that it can achieve higher frequency than others acoustic waves propagation technologies. The different characteristics of these resonators are mainly determined by their dimensions and the properties of the piezoelectric membrane.

Lithium Niobate has shown interesting piezoelectric properties such as a high phase velocity and large electromechanical coupling which enable wider filter bandwidths. Therefore, using this material in the XBAR represents an attractive way to respond to this flourishing need.

The aim of this project is thus to explore the potential of using LiNbO3 substrate with a new orientation. The case of a 128° Y-cut Lithium Niobate LiNbO3 membrane is going to be studied. For that we are first going to review the proprieties of the 128° Y-cut material and how the resonator composed of this substrate has been modeled. Finally, we will search for the combination of geometrical parameters which permits the optimal performance of the resonator.

2 Material properties of 128° Y-cut Lithium Niobate

First of all, exploring different orientations and cuts of the Lithium Niobate is easily accessible because of its commercial availability, which enables its production. Thus, after simulating the behavior of the resonator composed of this substrate, we can compare the results from the theory to the experimentation.

Lithium Niobate belongs to the trigonal crystal system, which can be characterized by both an hexagonal and a rhombohedral unit cell. It is classified as a piezoelectric material, which also means it has anisotropic features. Depending on the orientation its properties are going to be different. The piezoelectric coupling matrix (e), the elastic stiffness matrix (c) and the relative permittivity (ϵ) of the material in a standard orientation are the following.

$$e = \begin{bmatrix} 0 & 0 & 0 & 0 & 3.69 & -2.42 \\ -2.42 & 2.42 & 0 & 3.69 & 0 & 0 \\ 0.3 & 0.3 & 1.77 & 0 & 0 & 0 \end{bmatrix} (C/m^2)$$

$$c = \begin{bmatrix} 1.9839e11 & 5.4720e10 & 6.5130e10 & 7.880e9 & 0 & 0 \\ 5.4720e10 & 1.9839e11 & 6.5130e10 & -7.880e9 & 0 & 0 \\ 6.5130e10 & 6.5130e10 & 2.279e11 & 0 & 0 & 0 \\ 0 & 0 & 0 & 0 & 5.9650e10 & 7.880e9 \\ 0 & 0 & 0 & 0 & 7.880e9 & 7.1835e10 \end{bmatrix} (N/m^2)$$

$$\epsilon = \begin{bmatrix} 45.60 & 0 & \\ 0 & 45.6 & 0 \\ 0 & 0 & 45.6 \end{bmatrix}$$

The rotation around the x-axis of 38° as shown in the figure 1 allows to find the new properties of 128° Y-cut material.

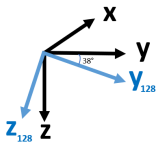

Figure 1: Rotation

$$e = \begin{bmatrix} 0 & 0 & 0 & 0 & 4.40 & 0.36 \\ -1.72 & 4.53 & 1.35 & 0.22 & 0 & 0 \\ 1.73 & -2.45 & 2.60 & 0.74 & 0 & 0 \end{bmatrix} (C/m^2)$$

$$c = \begin{bmatrix} 1.98e11 & 6.63e10 & 5.35e10 & 6.96e9 & 0 & 0 \\ 6.63e10 & 1.87e11 & 8.05e10 & 6.31e9 & 0 & 0 \\ 5.35e10 & 8.05e10 & 2.09e11 & 6.01e9 & 0 & 0 \\ 0 & 0 & 0 & 0 & 5.66e10 & -4.05e9 \\ 0 & 0 & 0 & 0 & -4.01e9 & 7.49e10 \end{bmatrix} (N/m^2)$$

$$\epsilon = \begin{bmatrix} 45.60 & 0 & \\ 0 & 38.18 & -9.36 \\ 0 & -9.36 & 33.62 \end{bmatrix}$$

It has been shown that resonator with LiNbO3 have wider frequency band and higher electro-mechanical coupling (k^2) due to the larger value of the component $e15$ of the coupling matrix and its value increase for the 128° Y-cut ($e15_{LiNbO3} = 3.69\ C/m^2$ *and* $e15_{LiNbO3_{128}} = 4.40\ C/m^2$). We therefore expect to obtain even wider frequency band for this specific orientation of the material.

3 XBAR Resonator 2D model

The XBAR resonator has been designed by a 2D model, which is based on the fact that its behavior mainly depends on the dimensions along (X, Z) plane, which are regrouped in table 1. The device is a repetition of electrode pairs, as we can see in the figure 2. Therefore, we can consider a single pair simulation and apply periodic boundary conditions on the right and left side to simulate the periodicity.

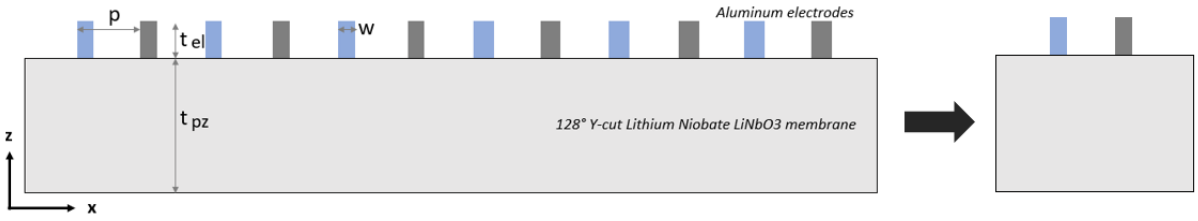

Figure 2: Schematic front view of the resonator

Symbol	Definition	Dimension
t_{pz}	piezoelectric thickness	$0.4\mu m$
t_{el}	electrode thickness	μm
w	electrode width	μm
p	pitch	μm

Table 1: Geometrical parameters

The thickness of the Lithium Niobate t_{pz} is fixed, because the membrane is directly provided by a manufacturer. Therefore, we can optimise the combination of the thickness and width of the electrodes and the pitch. The COMSOL© model used for that purpose is described in the following parts.

3.1 Physics of the model

The simulation of a resonator is a multi-physic problem which requires the coupling of 'Solid Mechanics' and 'Electrostatics' models.
The deformation of the piezoelectric material is induced by the difference of potential applied on the electrode, 0V and 1V.
The resonator model is represented in figure 3, and is divided is 3 areas, represented by different colors.
- The blue one represents the air around the component,
- the pair of electrode is colored in red,
- and the piezoelectric membrane in pink.

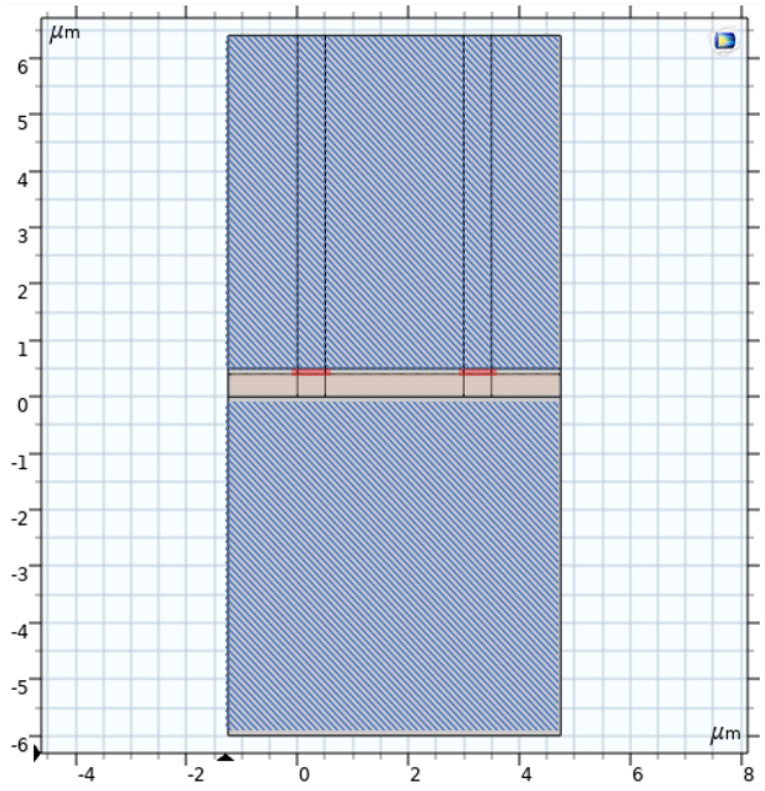

Figure 3: COMSOL© model

The different sections of the model (Air, Aluminium, 128° Y-cut Lithium Niobate) have specific properties and as a results, the physics applied are going to be different.
First of all, the 'Electrostatics physic' is valid in the whole domain whereas 'Solid Mechanics physic' is only applied on the resonator (Al + LiNbO3).
The difference of potential that induces the deformation of the piezoelectric membrane creates an electric field, and thus a set of equations are required to link it with the different domains properties. The 'Charges conservation' which relates the electric displacement D (according to Gauss's law) with the electric field E and the associated properties of the domain (*such as the relative permittivity*) is used in all three domain separately.

3.2 Initial conditions

Initial conditions describes the physics at t=0 s, and we set no displacement field, no structural velocity field and no electric potential.

3.3 Boundary conditions

As we have seen, the model only represents a pair of electrode, we thus use periodic boundary condition on the right and left side of the whole domain.

3.4 Materials

The Lithium Niobate is modeled by the 'Piezoelectric Material' function and naturally the Aluminium of the electrode by 'Linear Elasticity'. In order to visualize Y-cut, the component $e15$ of the piezoelectric coupling matrix should represent the electric field in the 1(X) direction and the shear in 5(XZ) direction. Therefore, the plane in which we will use the piezoelectric material is (X, Z).

3.5 Mesh

The design of the resonator is only composed of rectangles of different size. Thus, the adapted mesh type is structured with orthogonal quadrilateral elements. The Mesh also need to be mapped in different location with various distribution in order to refine close to the electrode and the piezoelectric membrane, where accuracy is needed in order to have consistent results.
The size of the distributions therefore depends on the geometrical parameters, with a maximum element size of 1.1μm, a minimum element size of 0.00492μm, a maximum element growth rate of 1.3 and a curvature factor of 0.3. The Mesh is represented in figure 4.

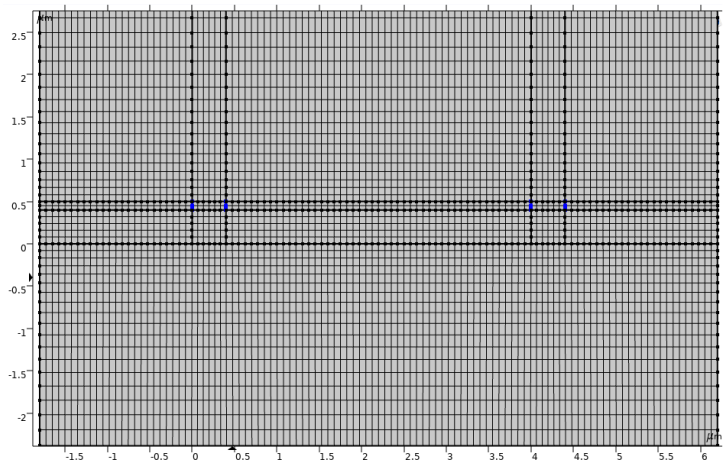

Figure 4: COMSOL© model's mesh

3.6 Frequency range

In order to have a good visualisation of the results and frequency response of the resonator, we have to consider a range of frequency which is $-2\Delta f \leqslant \mathrm{f} \leqslant 2\Delta f$. Where $\Delta f = f_s - f_p$, with f_s the frequency with the maximum admittance which is the resonance and f_p the frequency with the minimum admittance, the anti-resonance.
This condition has always to be satisfy, for that we take $3000 \leqslant f \leqslant 7000$ MHz.

4 Comparison with the literature

For the purpose of the optimisation of the geometrical parameters, we first have to check the validity of our model, for that we can compare it to the excited literature. A study has already been done on XBAR with 128° Y-cut Lithium Niobate LiNbO3 membrane with Aluminum electrodes on top : *'A1 Resonators in 128° Y-cut Lithium Niobate with Electromechanical Coupling of 46.4%. Journal of Microelectromechanical Systems'* [LYLG20]. Therefore, we can compare our results with it, using the same values of pitch, thickness and width. However, we have to be aware of the fact that the material properties and losses are slightly different, and the device was modeled by

multiple electrodes. Nevertheless if the assumptions made to develop our model are correct, the results obtain in both case should be close.

4.1 Model

The FEM model of the article is also 2D and corresponds to the schematic b in the figure 5. The device in the article which corresponds to our case is the device A (see table 2 and figure 6).

t_{pz}	t_{el}	w_{el}	p
$550nm$	$300nm$	$3\mu m$	$20\mu m$

Table 2: Geometrical parameters of [LYLG20] model's

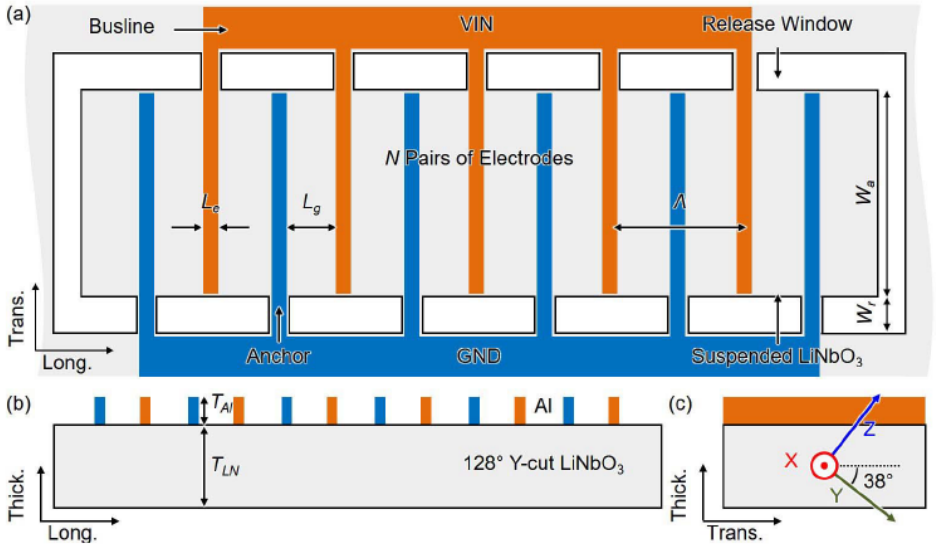

Figure 5: Schematic model extracted from figure 2 [LYLG20]

Sym.	Parameter	Value	Sym.	Parameter	Value
Λ	Cell length (μm)	20-40	W_a	Aperture width (μm)	65
L_e	Electrode length (μm)	3-4	W_r	Release window width (μm)	8
L_g	Gap length (μm)	6-17	T_{LN}	$LiNbO_3$ thickness (nm)	550
N	No. of electrode pairs	5-10	T_{Al}	Aluminum thickness (nm)	300

Design	Λ (μm)	L_e (μm)	L_g (μm)	N (μm)	W_a (μm)
Device A	40	3	17	5	65
Device B	30	4	11	5	65
Device C	20	4	6	10	65

Figure 6: Geometrical parameters of the literature's model extracted from TABLE I and TABLE III [LYLG20]

4.2 Results

Using the geometrical parameters given in the section below, we obtain the following admittance-frequency curves in figure 7, where the (a) is the one from [LYLG20] and (b) our simulation.

Both curves have the same shape and the main pics are represented. Indeed, the excited modes around 2.5 GHz are present in both case, and the ones close to the resonance and anti-resonance are also part of their response.
The resonance and anti-resonance frequency we obtain have less than 1% difference with the literature, which is justify by simulation models and material properties particularity. The table 3 regroups the different values of f_p, f_s and quality factor of the two studies.

The amplitude on the pics are slightly different because the y-axis is in decibel for the plot of the article and logarithmic (Siemens) in our case.

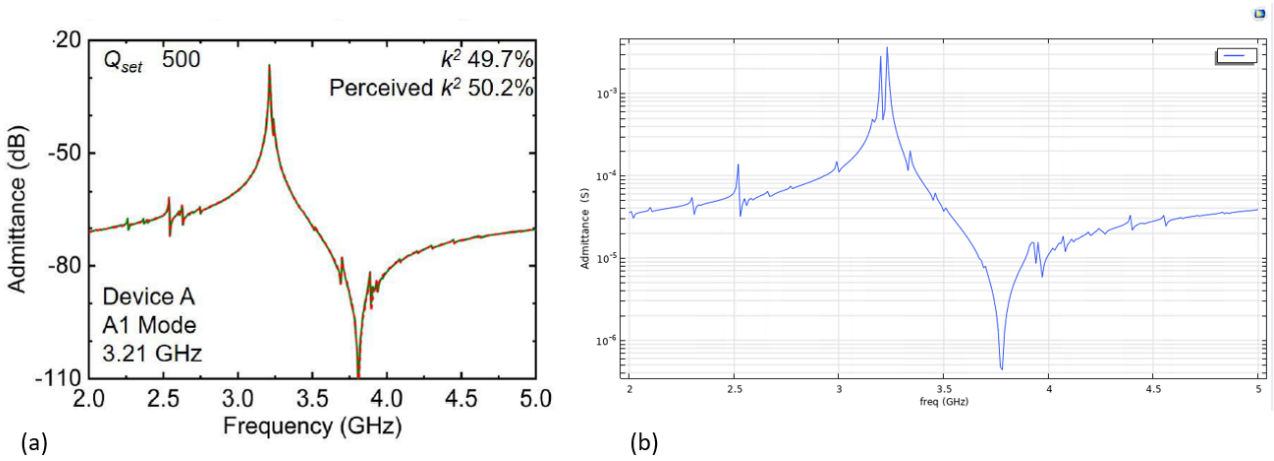

Figure 7: Comparison of the admittance, (a) corresponds to the model [LYLG20] and (b) to our simulation

Model	Resonance frequency f_s	Anti-resonance frequency f_p	$k^2_{perceived}$*
Project	3.23 GHz	3.78 GHz	45.6%
Article	3.21 GHz	3.81 GHz	50.2%

Table 3: Comparison of the results

* The electromechanical coupling perceived is calculated the following way.
$k^2_{perceived} = \frac{\pi^2}{8}((\frac{f_p}{f_s})^2 - 1)$

Before we can give a conclusion on the validity of our model, we have to look at the displacement field and stress tensor of the models, to have a more accurate comparison of them.

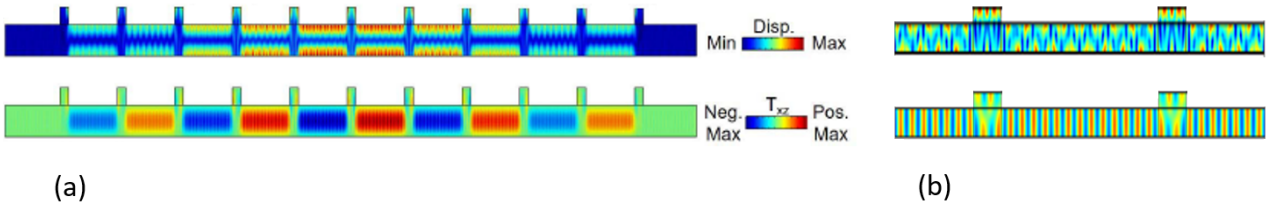

Figure 8: Comparison of the total displacement and the stress tensor component xz, (a) corresponds to the model [LYLG20] and (b) to our simulation

According to the figure 8, we can see that if we further compress the figure b, we obtain a similar behavior than the article's resonator between two electrodes.
For the stress tensor component xz, we identify the succession of vertical red line of high stress for both case. The displacement also shows similarity. The maximum is located on the top and bottom of the piezoelectric membrane and the minimum displacement is in between.

Finally, we can conclude that our model is valid for pairs of electrodes that are far from the sides end of the resonator (at least after 2 pairs of electrodes). Therefore, we can study the optimisation of the geometrical parameters.

5 Optimisation of the geometrical parameters

As we have seen, the aim is to find the combinations of parameters (*pitch, electrode thickness and width*) which allows to have the optimal performance of the resonator. It means that the electromechanical coupling has to be the highest possible but in the same the resonator should have limited numbers of excited modes.
The electromechanical coupling k^2 can be estimated using the following relation.

$$k^2 \propto \frac{f_p - f_s}{f_p} = \frac{\Delta F}{F} \tag{1}$$

Therefore, we are first going to study the impact of the pitch variation for a fixed electrode geometry. In a second hand, we will understand the consequences of the width variation. And finally the influence of the electrode's thickness.
Those studies will thus allow us to find the optimal parameters combinations.

5.1 Pitch variation

In order to study the impact of the pitch variation, the geometry of the electrode is fixed, we have $t_{el} = 0.1\mu m$ and $w_{el} = 0.5\mu m$.

$$\text{p} = \{2\ 3\ 4\ 5\ 6\ 10\}\ \mu m$$

Using the 'parametric sweep' option of COMSOL©, we can have the results of the sweep of the pitch in the same time (*as the numbers of variations is only 6, the software memory is not full*). The results are given in the table in the following figure 9.

P (µm)	fs(GHz)	Y(S)	fp(GHz)	Y(S)	ΔF(Hz)	ΔF/F (%)	Numbers of modes
2	4,997	0,0645	5,711	1,15E-06	714	12,50	3
3	4,746	0,0365	5,545	6,78E-07	799	14,41	5
4	4,637	0,0256	5,467	5,02E-07	830	15,18	5
5	4,577	0,0263	5,416	4,11E-07	839	15,49	6-7
6	4,541	0,0243	5,380	3,51E-07	839	15,59	7
10	4,475	0,0144	5,277	2,40E-07	802	15,20	6-7

Figure 9: Resonance and anti-resonance frequency, electromechanical coupling and numbers of modes for different pitch

We can notice that resonance frequency is influenced by the value of the pitch.

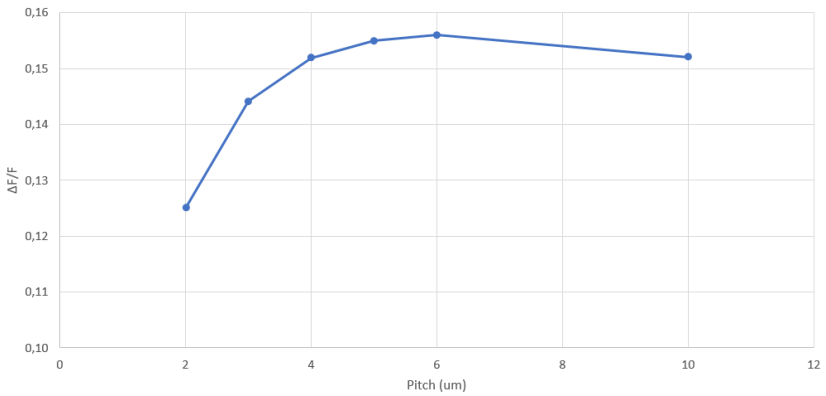

Figure 10: Evolution of $\Delta F/F$ for different pitch and fixed electrode geometry

From the results display in the table figure 9 and the figure 10 above, we can conclude that, the number of excited modes and the electromechanical coupling increase with higher values of pitch. However, the electromechanical coupling start decreasing for $p \geq 6\mu m$ and the gain is more important for smaller pitch.
The electrode width and thickness used to understand the impact of the pitch variation are probably not appropriate for important pitch such as $10\mu m$.

The admittance graph obtained for this study are presented bellow in figure 11.

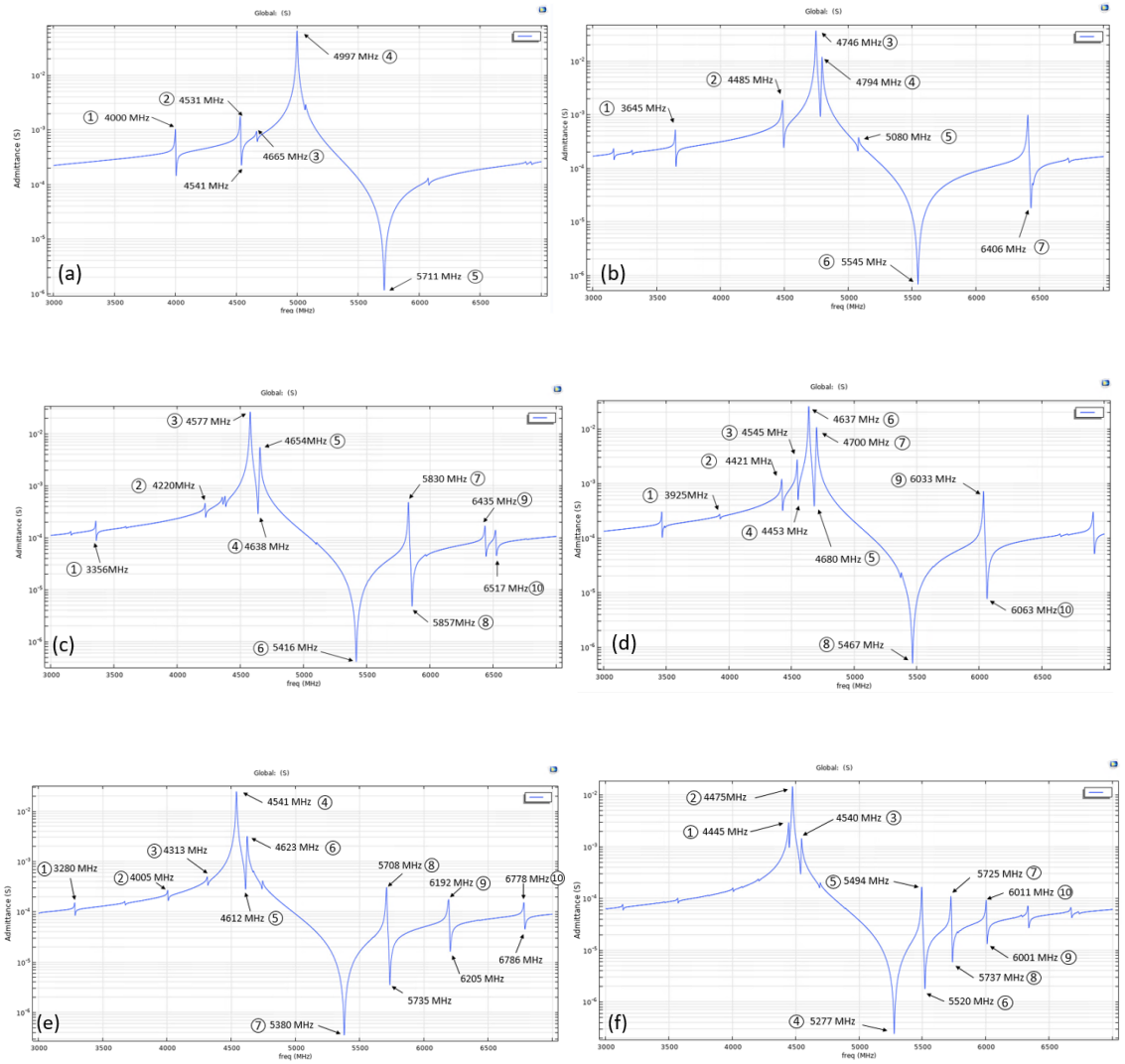

Figure 11: Admittance curve with pics frequency for (a) $p = 2\mu m$, (b) $p = 3\mu m$, (c) $p = 4\mu m$, (d) $p = 5\mu m$, (e) $p = 6\mu m$, (f) $p = 10\mu m$

For these geometrical parameters, the results are not convenient. Indeed, the criteria on the electromechanical coupling is fulfil because we have wide band frequency but the number of excited modes are too important and expect for $p = 2\mu m$ there are harmonics close to the resonance and anti-resonance, which is not acceptable for the design of a resonator.

Finally, increasing the pitch for a fixed t_{el} and w_{el}, decreases the frequency of the resonance and disturb the response of the resonator, as the number of excited modes increases.

5.2 Electrode width variation

We will now study the response of the resonator for different electrode width and a fixed thickness $t_{el} = 0.1\mu m$.

$$w_{el} = \{0.5\ 0.75\ 1\ 1.5\ 2\}\ \mu m$$

First of all, we are going to analyse the case of one pitch for example $p = 5\mu m$ and we will then globally look at the influence of the width for the other pitch p $=\{2\ 3\ 4\ 6\ 10\}\ \mu m$.

5.2.1 Case study $p = 5\mu m$

The admittance curves presented below for the different width, prove that increasing the electrode width excite an important number of modes and their amplitude become greater.
Contrary to the pitch variations, small width increments have an important impacts on the behavior of the device.

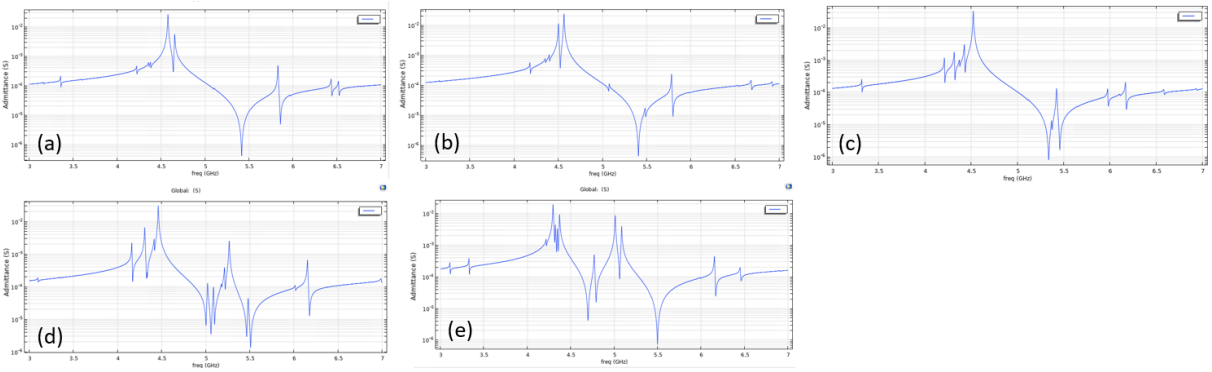

Figure 12: Admittance curves for (a) $w_{el} = 0.5\mu m$, (b) $w_{el} = 0.75\mu m$, (c) $w_{el} = 1\mu m$, (d) $w_{el} = 1.5\mu m$, (e) $w_{el} = 2\mu m$

On the other hand the electromechanical coupling is also more important for larger electrode width as we can see in the table represented in figure 13.
Therefore, we have to find a compromise between important electromechanical coupling and number of modes. Reducing the pics is the most important criteria. Indeed, because of their important presence the behaviour of the resonators makes it unusable. Large electromechanical coupling is a further improvement but the proper functioning of the device is mostly based on its admittance response.

p = 5 µm

Wel (µm)	fs(GHz)	Ymax(S)	fp(GHz)	Ymin(S)	ΔF/F (%)	Numbers of modes
0,5	4,577	0,0263	5,416	4,109E-07	15,49%	6
0,75	4,563	0,0234	5,405	4,310E-07	15,58%	8
1	4,522	0,033	5,337	8,068E-07	15,27%	10
1,5	4,461	0,0297	5,508	1,333E-06	19,01%	12
2	4,296	0,019	5,498	7,304E-07	21,86%	12

Figure 13: Resonance and anti-resonance frequency, electromechanical coupling and numbers of modes for different electrode width

We can remark that the resonance frequency is less influenced by the width sweep than the pitch variation.

5.2.2 Overview for different pitch

The diagram figure 14 in which we have the number of modes for the width sweep for all pitch that we study allow us to conclude that all pitch have the same trend. The number of excited modes increases with the width. The value of this number becomes too important when the $w_{el} > 0.75\mu m$.

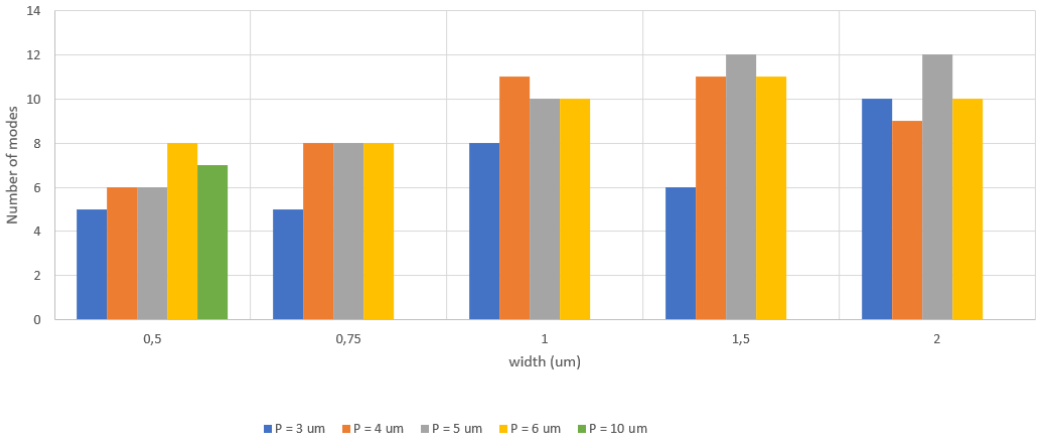

Figure 14: Evolution of the number of modes for increasing electrode width and pitch

As we have seen trying to reduce the numbers and the importance of theses pics is our most important concern, but we can still look at the evolution of the electromechanical coupling which is represented in the following graph figure 15.

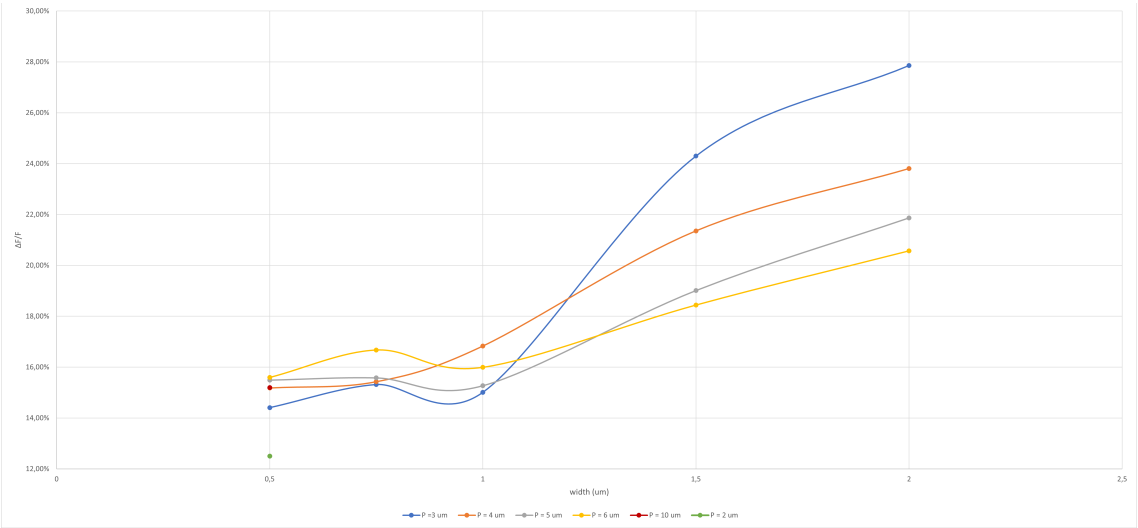

Figure 15: Evolution of the electromechanical coupling for the electrode width sweep for different pitch

Moreover, as we can notice on the graph 15, for $p = 2$, the evolution was not plotted when $w > 0.75\mu m$ due to geometrical constraint of the model.

For smaller width, bigger pitch have more important electromechanicl coupling, however this trend start reversing when w_{el} becomes larger than 1 μm. This inversion of trend happen when $0.75\mu m \leqslant w_{el} \leqslant 1.25\mu m$.

The admittance graph obtained for the different pitch are presented bellow in figure 16, 17, 18, 19 and 20.

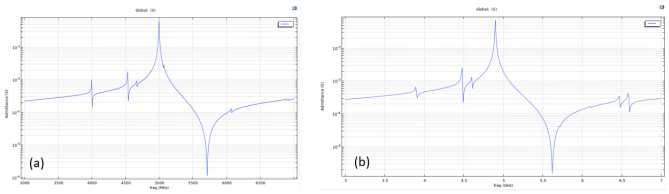

Figure 16: Admittance curve of $p = 2\mu m$ and $t_{el} = 0.1\mu m$ for (a) $w_{el} = 0.5\mu m$, (b) $w_{el} = 0.75\mu m$

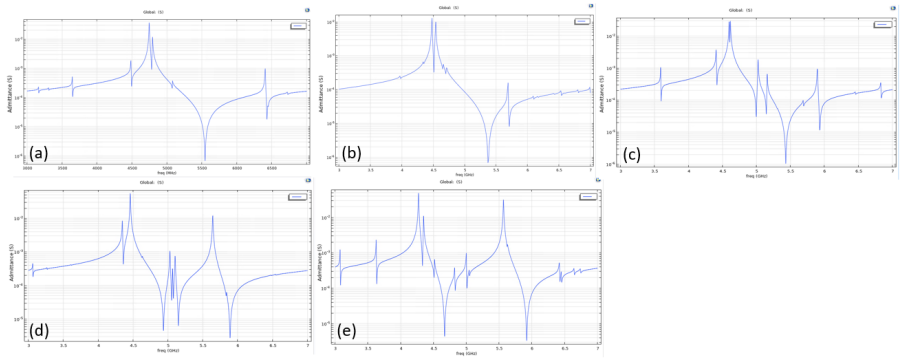

Figure 17: Admittance curve of $p = 3\mu m$ and $t_{el} = 0.1\mu m$ for (a) $w_{el} = 0.5\mu m$, (b) $w_{el} = 0.75\mu m$, (c) $w_{el} = 1\mu m$, (d) $w_{el} = 1.5\mu m$, (e) $w_{el} = 2\mu m$

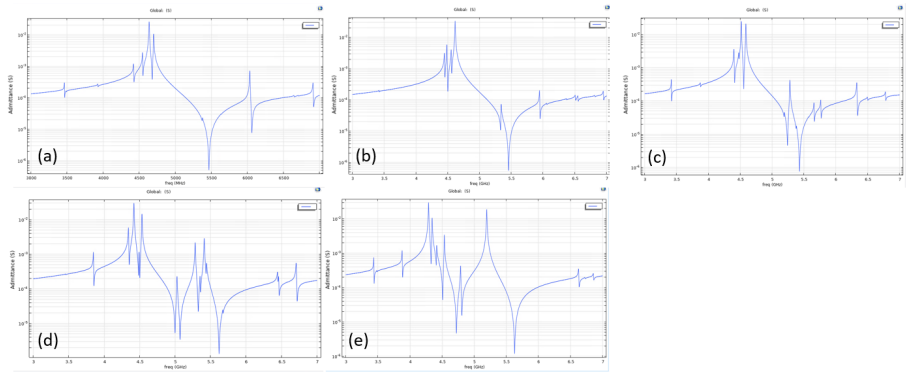

Figure 18: Admittance curve of $p = 4\mu m$ and $t_{el} = 0.1\mu m$ for (a) $w_{el} = 0.5\mu m$, (b) $w_{el} = 0.75\mu m$, (c) $w_{el} = 1\mu m$, (d) $w_{el} = 1.5\mu m$, (e) $w_{el} = 2\mu m$

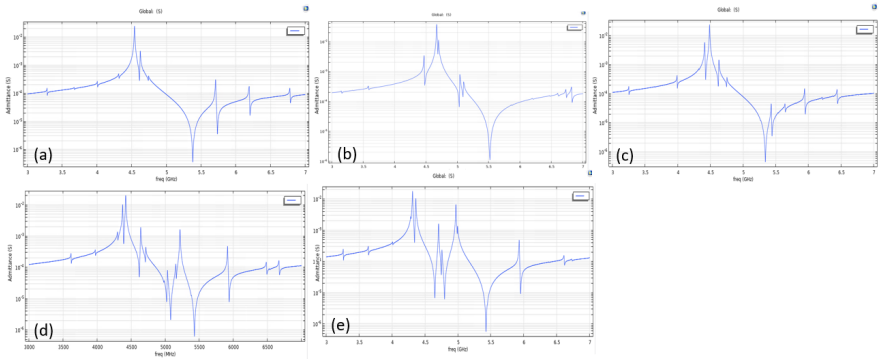

Figure 19: Admittance curve of $p = 6\mu m$ and $t_{el} = 0.1\mu m$ for (a) $w_{el} = 0.5\mu m$, (b) $w_{el} = 0.75\mu m$, (c) $w_{el} = 1\mu m$, (d) $w_{el} = 1.5\mu m$, (e) $w_{el} = 2\mu m$

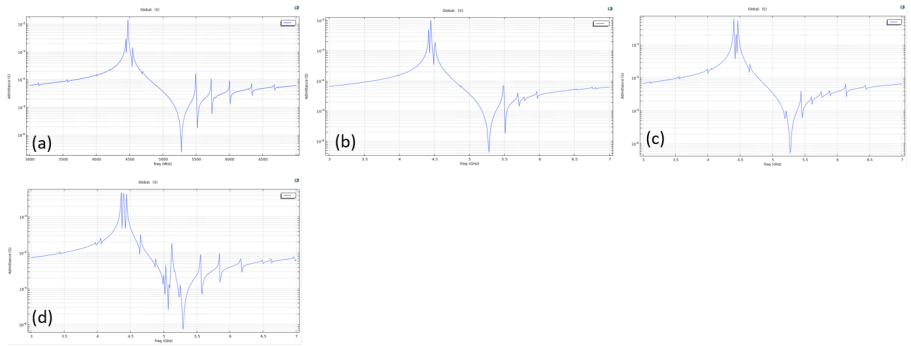

Figure 20: Admittance curve of $p = 10\mu m$ and $t_{el} = 0.1\mu m$ for (a) $w_{el} = 0.5\mu m$, (b) $w_{el} = 0.75\mu m$, (c) $w_{el} = 1\mu m$, (d) $w_{el} = 1.5\mu m$

All the parameters combinations in figures 17, 18, 19 and 20, can not be use to produce filters. When $w_{el} < 0.75\mu m$, the numbers of pics and their amplitude are correct but can be improved, however their locations is unacceptable because they are close to either the resonance or anti-resonance. Whereas when $w_{el} \geq 0.75\mu m$ the number of excited mode is the problem.

Finally, more the width increases, more we have harmonics until the behavior of the resonators is unusable because we can barely distinguish the resonance and anti-resonance and in addition the amplitude of the pics also becomes greater.
Therefore, in order to find the best combination of parameters we have to focus on width smaller than $0.75\mu m$.

$$w_{el} \leqslant 0.75\mu m \tag{2}$$

5.3 Electrode thickness variation

We have seen that increasing the width has a bigger impact on the admittance response of the resonator than increasing the pitch. We will therefore, explore the influence of electrode thickness changes $t_{el} = \{$ 0.1 0.15 0.2 0.25 0.3$\}$, for a fixed width $w_{el} = 0.5\mu m$.

5.3.1 Case study $p = 5\mu m$

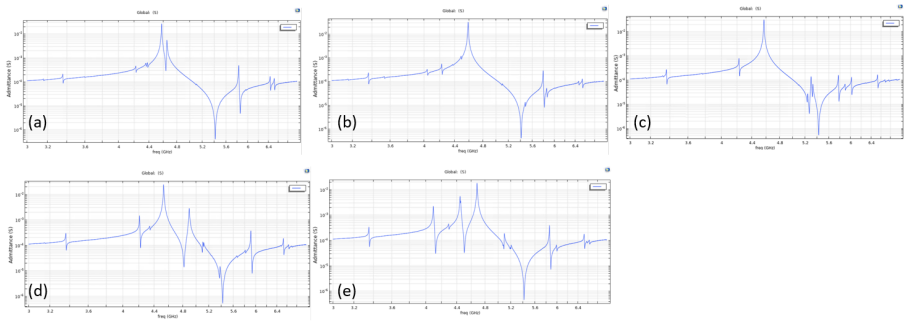

Figure 21: Admittance curve of $p = 5\mu m$ and $w_{el} = 0.5mum$ for (a) $t_{el} = 0.1\mu m$, (b) $t_{el} = 0.15\mu m$, (c) $t_{el} = 0.2\mu m$, (d) $t_{el} = 0.25\mu m$, (e) $t_{el} = 0.3\mu m$

Analysing the admittance-frequency curves for the case of $p = 5\mu m$ in figure 21, leads to the same conclusion as for the width. Therefore, in order to have a appropriate device, the thickness in this case should be inferior to $2\mu m$: $t_{el} \leq 0.2\mu m$.

Increasing the electrode thickness also impact the electromechanical coupling. Indeed, referring to figure 22, $\Delta F/F$ slightly decreases when $t_{el} = 0.15\mu m$, but in the same time this value gives the admittance frequency curve with the most convenient shape.

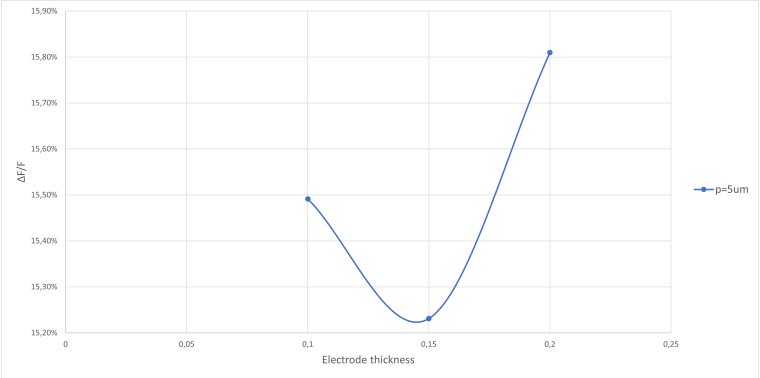

Figure 22: Evolution of the electromechanical coupling depending on the electrode thickness

p = 5 µm

tel (µm)	fs(GHz)	Ymax(S)	fp(GHz)	Ymin(S)	ΔF/F (%)
0,1	4,577	0,0263	5,416	4,109E-07	15,49%
0,15	4,586	0,0323	5,410	4,310E-07	15,23%
2	4,569	0,0315	5,427	5,338E-07	15,81%

Figure 23: Resonance and anti-resonance frequency, electromechanical coupling for different electrode thickness

For the specific case of $p = 5\mu m$, the electrode thickness should be $t_{el} \leq 0.2\mu m$, and especially $t_{el} = 0.15\mu m$ gives promising results. Therefore, we want to know if the fact that the thickness should be inferior to $2\mu m$ and that for $t_{el} = 0.15\mu m$ the behavior of the resonator is better than the other values explored, is also correct for the other pitch.

5.3.2 Overview for different pitch

In order to visualize the evolution of the response of the resonator, the admittance-frequency curves for for each pitch and width variation are represented bellow in figure 24, 25, 26, 27 and 28.

The results obtain for $p = 5\mu m$ are also valid for all the different pitch :
- the admittance response becomes exploitable for $t_{el} > 0.2\mu m$,
- $t_{el} = 0.15\mu m$ provides the most stable behavior,
- increasing t_{el} make the device unusable.

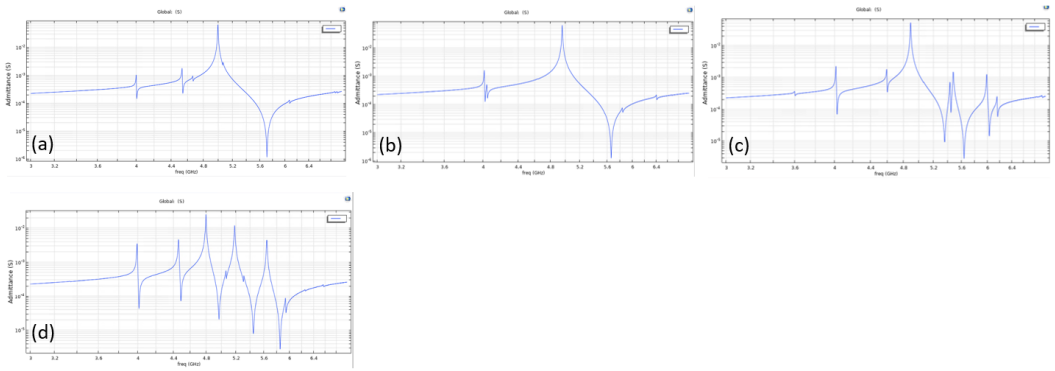

Figure 24: Admittance curve of $p = 2\mu m$ and $w_{el} = 0.5\mu m$ for (a) $t_{el} = 0.1\mu m$, (b) $t_{el} = 0.15\mu m$, (c) $t_{el} = 0.2\mu m$, (d) $t_{el} = 0.25\mu m$, (e) $t_{el} = 0.3\mu m$

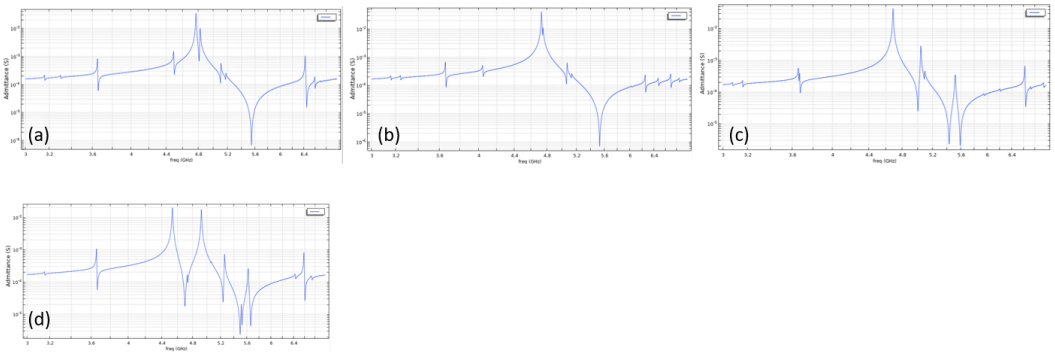

Figure 25: Admittance curve of $p = 3\mu m$ and $w_{el} = 0.5\mu m$ for (a) $t_{el} = 0.1\mu m$, (b) $t_{el} = 0.15\mu m$, (c) $t_{el} = 0.2\mu m$, (d) $t_{el} = 0.25\mu m$, (e) $t_{el} = 0.3\mu m$

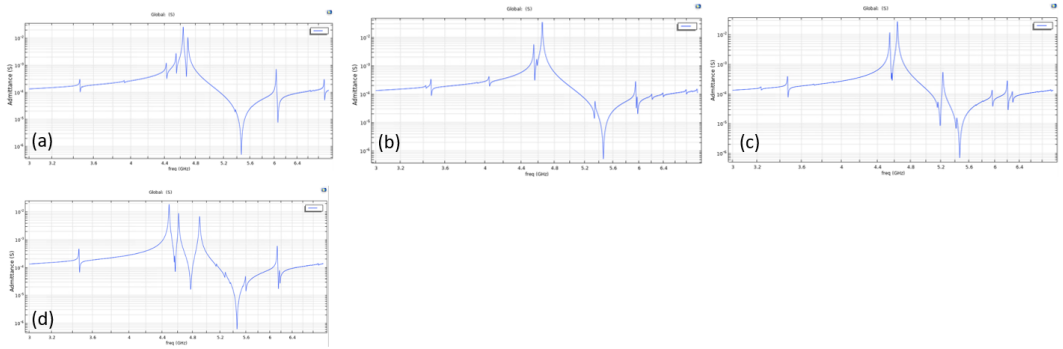

Figure 26: Admittance curve of $p = 4\mu m$ and $w_{el} = 0.5\mu m$ for (a) $t_{el} = 0.1\mu m$, (b) $t_{el} = 0.15\mu m$, (c) $t_{el} = 0.2\mu m$, (d) $t_{el} = 0.25\mu m$, (e) $t_{el} = 0.3\mu m$

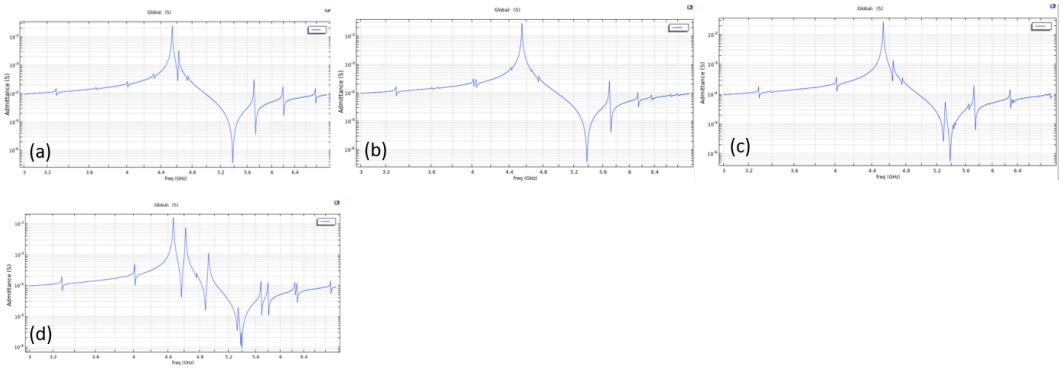

Figure 27: Admittance curve of $p = 6\mu m$ and $w_{el} = 0.5\mu m$ for (a) $t_{el} = 0.1\mu m$, (b) $t_{el} = 0.15\mu m$, (c) $t_{el} = 0.2\mu m$, (d) $t_{el} = 0.25\mu m$, (e) $t_{el} = 0.3\mu m$

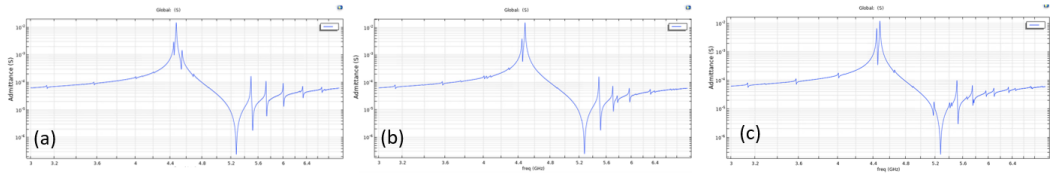

Figure 28: Admittance curve of $p = 10\mu m$ and $w_{el} = 0.5\mu m$ for (a) $t_{el} = 0.1\mu m$, (b) $t_{el} = 0.15\mu m$, (c) $t_{el} = 0.2\mu m$

In an other hand, increasing the electrode thickness also impact the electromechanical coupling. As we can see in figure 29, $\Delta F/F$ slightly decrease for t_{el} (as we have seen with $p = 5\mu m$). Nevertheless, the electromechanical coupling is still high compared to resonator with other piezoelectric materials.

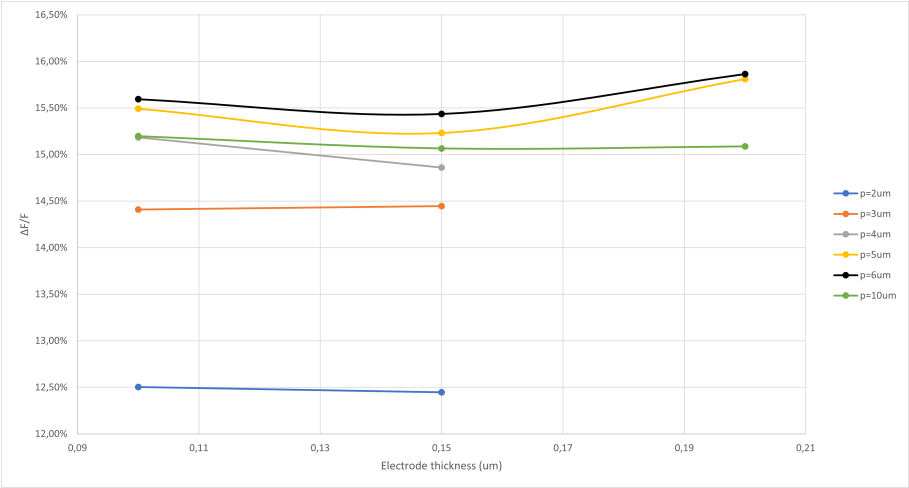

Figure 29: Evolution of the electromechanical coupling with the electrode thickness for different pitch*

** For p = 2, 3, 4 μm the electromechanical coupling are not plotted for electrode thickness bigger than 0.15 μm because as we can see in figure 24, 25, 26 we could not create resonators with $t_{el} > 0.75\mu m$, thus measuring it is not necessary.*

Moreover, the electrode thickness has also a bigger influence on smaller pitch. For example, the different thickness do not influence significantly the response of the resonator when $p = 10\mu m$, and the variation of electromechanical coupling is not important as well.

Finally, all these results lead us to the conclusion that, in general, for further improvement, we have to take an electrode thickness which is smaller than $0.2\mu m$.

$$t_{el} \leqslant 0.2\mu m \tag{3}$$

And the electrode thickness $t_{el} = 0.15\mu m$, has to be studied combined with appropriate width in order to find optimal results as the following combinations are already interesting to design resonators.
-$p = 2\mu m$, $w_{el} = 0.5\mu m$ $t_{el} = 0.1\mu m$ and $0.15\mu m$,
-$p = 6\mu m$, $w_{el} = 0.5\mu m$ $t_{el} = 0.15\mu m$,
-$p = 3\mu m$, $w_{el} = 0.5\mu m$ $t_{el} = 0.15\mu m$,
-$p = 5\mu m$, $w_{el} = 0.5\mu m$ $t_{el} = 0.15\mu m$,

5.4 Optimal combinations (t_{el} and w_{el}) for each pitch

We have studied the impact of all the different geometrical parameters (p, t_{el}, w_{el}) on the resonator. We arrive to the conclusion that $t_{el} \leqslant 0.2\mu m$ and $w_{el} \leqslant 0.75\mu m$ in order to obtain proper functioning devices. (And especially $t_{el} = 0.15\mu m$ gives interesting results we should explore).
Therefore, we have to combine geometrical parameters that fulfil the previews conditions in order to obtain more stable behavior, that balance the number of excited modes.
For that, we will study each pitch { 2 3 4 5 6 10 } μm value separately and focus on smaller width { 0.4 0.5 0.6 0.7 0.75 } μm and electrode thickness { 0.1 0.15 0.2 } μm.

In the following studies, if some geometrical parameters are not presented, it is because it is obvious that they can not be used for the design of resonators because of the importance of excited modes.
Moreover, in the following figures the admittance-frequency graph in the same column have the same electrode width and in the same line, the same electrode thickness.

5.4.1 Modes identification

In order to find the best combination of geometrical parameters, modal analysis is an important point, because it allows to have a better understanding of the behavior of the device and we can try to find a way to eliminate unwanted modes or to push them out of the filter pass band.

In general filter composed with Lithium Niobate piezoelectric membrane with electrodes on top exited by a lateral field, as in our case, two types of modes are expected. Indeed, according to the article, [YPK+19] *'Analysis of XBAR resonance and higher order spurious modes'*, we expect high order harmonics of Lamb waves in the horizontal direction such as symmetric shear modes S and anti-symmetric one A as we can see in the following figure 30.

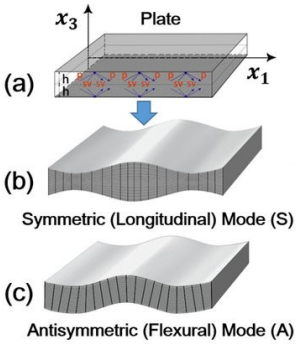

Figure 30: 'Lamb wave in a plate problem. (a) Geometry of the plate which is infinite in the x1 direction. (b) Compressional waves in a plate (symmetric mode). (c) Flexural waves in a plate (antisymmetric mode)' extraced from [SDL+18] *'Interaction of Lamb Wave Modes with Weak Material Nonlinearity : Generation of Symmetric Zero-Frequency Mode'*

5.4.2 p = 2 μm

Parameters combinations

We are first going to study the case of $p = 2\mu m$. Combining all the parameters define previously, we obtain the results in figure 31.

The two combinations of parameters (d) : $t_{el} = 0.15\mu m$, $w_{el} = 0.5\mu m$ and (e) : $t_{el} = 0.15\mu m$, $w_{el} = 0.4\mu m$ give satisfactory results, because there are only 2 excited modes that are not close to the resonance. In order to decide between them, the one with higher electromechanical coupling will be retain.
Thus, (d) : $t_{el} = 0.15\mu m$, $w_{el} = 0.5\mu m$ is the optimal geometrical parameter combination for $p = 2\mu m$.

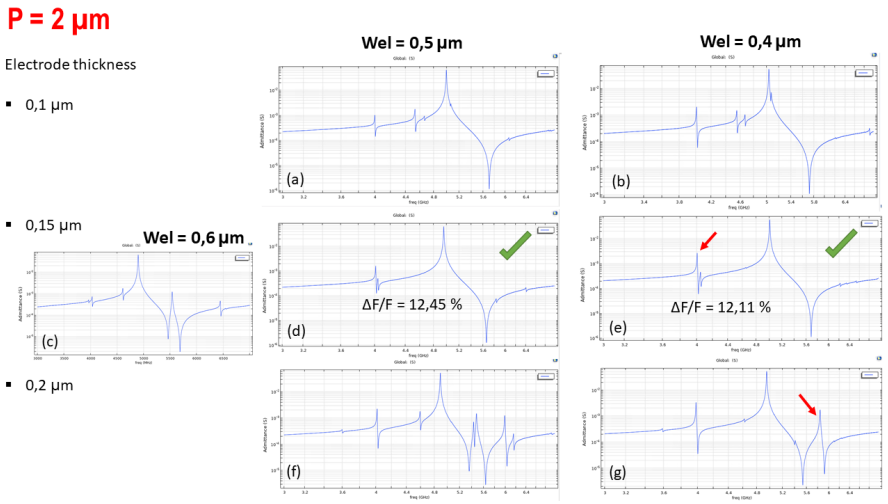

Figure 31: Admittance curves for different parameters combinations for $p = 2\mu m$

Modes identification

There are excited modes that remain for all the parameters sweep, represented by red arrows in figure 31. Therefore, we want to understand why they are exited, and which spurious modes they represent.

Analysing the displacement field, and some of the stress tensor component, we can identify that the remaining mode before the resonance is an $A0$ (see figure 32). This harmonic seems to disappear for increasing width, but new ones unfortunately come out with higher amplitude.

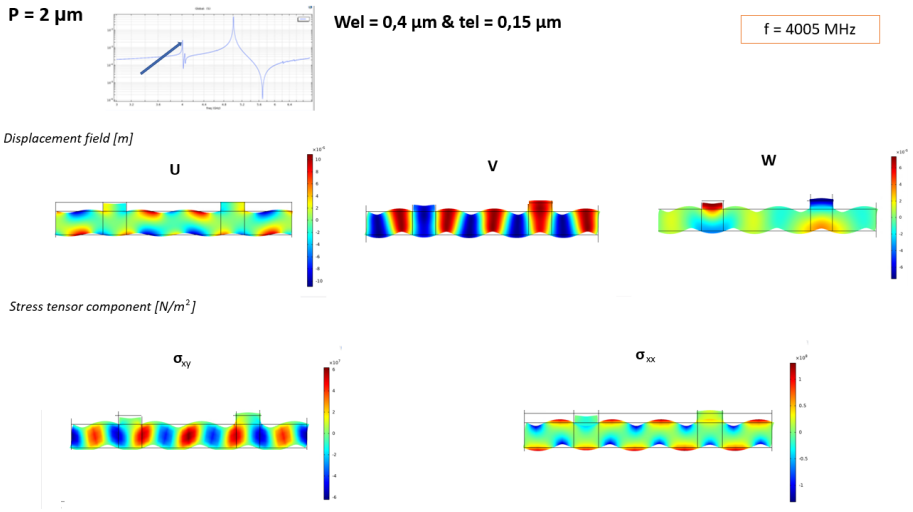

Figure 32: Displacement field and tensor stress to identify the spirious mode at f=4005Hz for $p = 2\mu m$, $w_{el} = 0.4\mu m$ and $t_{el} = 0.15\mu m$

Moreover, we also want to understand the reason why a high amplitude pic appears when the electrode thickness is $2\mu m$. It seems to be an SH1 (see figure 33).

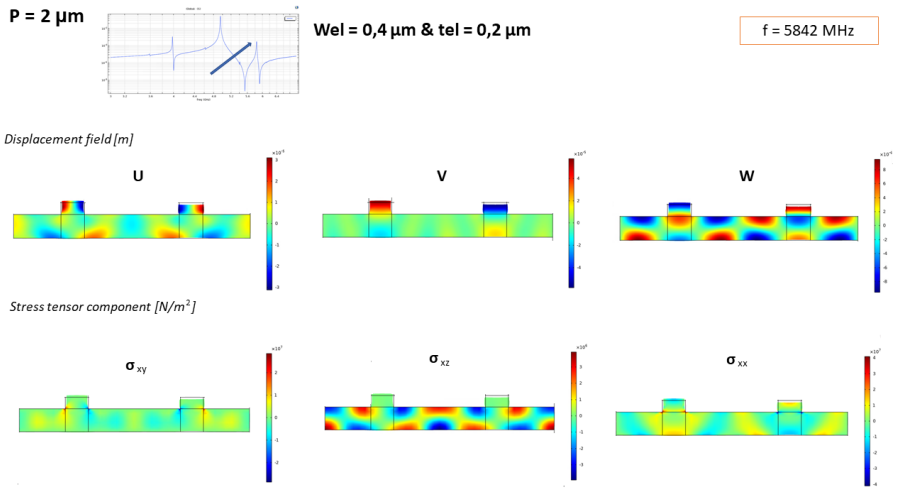

Figure 33: Displacement field and tensor stress to identify the spurious mode at f=5842Hz for $p = 2\mu m$, $w_{el} = 0.4\mu m$ and $t_{el} = 0.15\mu m$

In conclusion, for $p = 2\mu m$, the pre-resonance $A0$ spurious mode seems to disappears for smaller width with increasing thickness. Whereas for higher values of width and electrode thickness new symmetric modes appears after the anti-resonance and in between the two main pics.

Thickness proportionality $t_{pz} = t_{el}$

It is possible that, when the thickness of the electrode is equal to the thickness of the membrane (here $t_{pz} = t_{el} = 0.4\mu m$), some spurious modes disappear. However, looking at the admittance response of the filter in figure 34, the thickness proportionality do not permits to have better results. It does not reduce or eliminate the spurious modes but it actually add new ones.

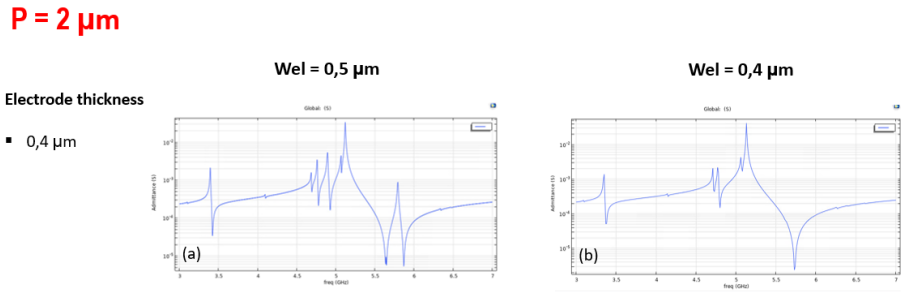

Figure 34: Admittance curves for $p = 2\mu m$, $t_{el} = 0.4\mu m$ and (a) $w_{el} = 0.5\mu m$, (b) $w_{el} = 0.4\mu m$

Finally, the optimal parameter combination for $p = 2\mu m$ is : $t_{el} = 0.15\mu m$ and $w_{el} = 0.5\mu m$.

We can also explore $p = 2\mu m$, $t_{el} = 0.15\mu m$ and $w_{el} = 0.4\mu m$, as the behavior is similar to the optimal one with a slightly higher mode amplitude and lower electromechanical coupling.

Unfortunately, no parameters combination permits to suppress the pre-resonance mode.

5.4.3 p = 3 μm

We will follow the same methodology as in the previews part for $p = 2\mu m$.

The admittance response for different parameters combinations, represented in figure 35 show that it also exists lasting excited modes such as :
- in between the resonance and anti-resonance, which amplitude becomes greater for increasing thickness,
- close in the pic of the main frequency, which disappears with increasing thickness and width.

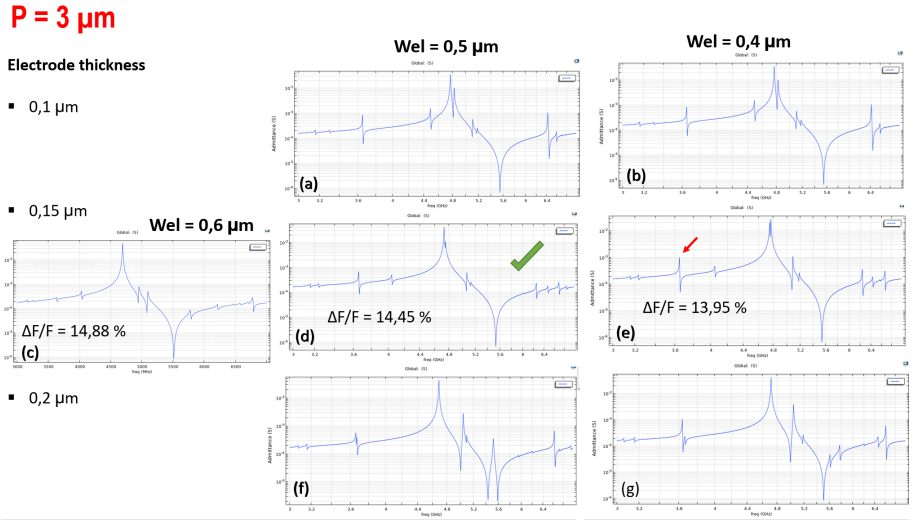

Figure 35: Admittance curves for different parameters combinations for $p = 3\mu m$

The combination $t_{el} = 0.15\mu m$ and $w_{el} = 0.5\mu m$ presents the best compromise between numbers of pics, their amplitude and location in the spectrum.

Nevertheless, we want to know the spurious type of the pre-resonance mode and the ones present midway between the resonance and anti-resonance.

Modes identification

The first excited mode in the spectrum, at a frequency $f < f_s$ is the same as for $p = 2\mu m$ and corresponds to $A0$ and tends to disappear for increasing thickness. However, it is difficult to have more detail on this mode.

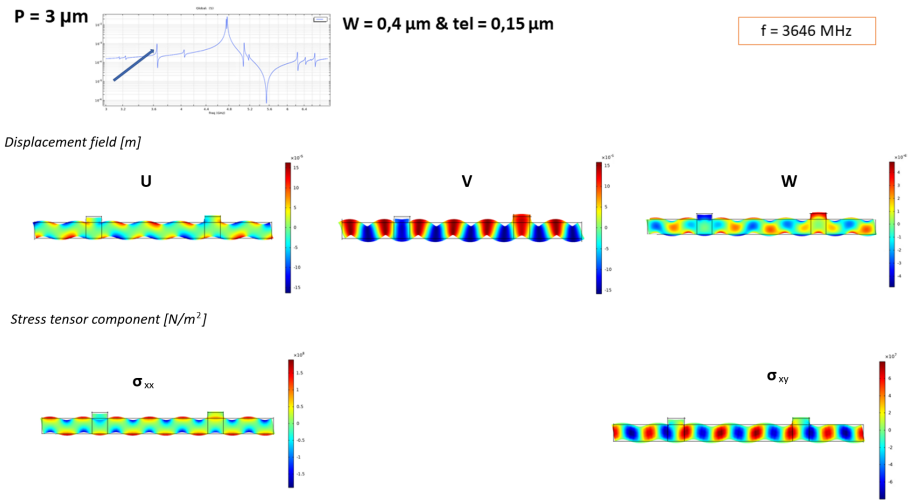

Figure 36: Displacement field and tensor stress to identify the spurious mode at f=3646Hz for $p = 3\mu m$, $w_{el} = 0.4\mu m$ and $t_{el} = 0.15\mu m$

In a other hand, the amplitude of the harmonics in between the resonance and anti-resonance decreases with smaller thickness and drastically increases for larger thickness. Their identification is non-trivial and did not gives known type modes, because they are extremely sensible to small parameters changes.

Thickness proportionality $t_{pz} = t_{el}$

As for $p = 2\mu m$, $t_{el} = t_{pz}$ does not reduce or eliminate disturbing spurious modes but it actually add new ones.

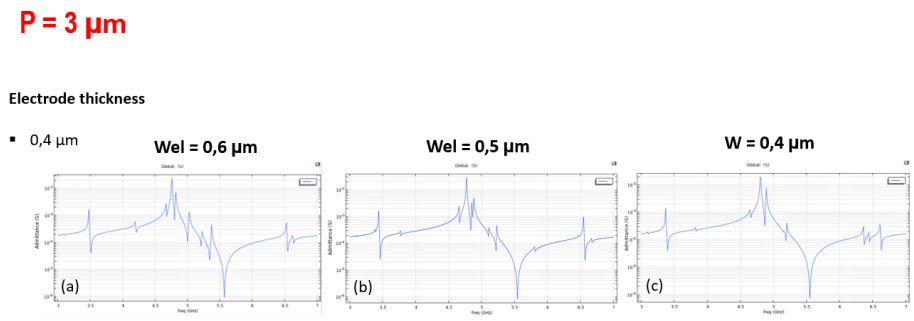

Figure 37: Admittance curves for $p = 3\mu m$, $t_{el} = 0.4\mu m$ and (a) $w_{el} = 0.6\mu m$, (b) $w_{el} = 0.5\mu m$, (c) $w_{el} = 0.4\mu m$

Finally, the optimal parameter combination for $p = 3\mu m$ is : $t_{el} = 0.15\mu m$ and $w_{el} = 0.5\mu m$.

5.4.4 p = 4 μm

Parameters combinations

For $p = 4\mu m$, as we can seen in the figure 38, for all parameters combinations, there are always harmonics close to either the resonance or anti-resonance, or both of them. The location of these harmonics is unacceptable to design functional resonators.

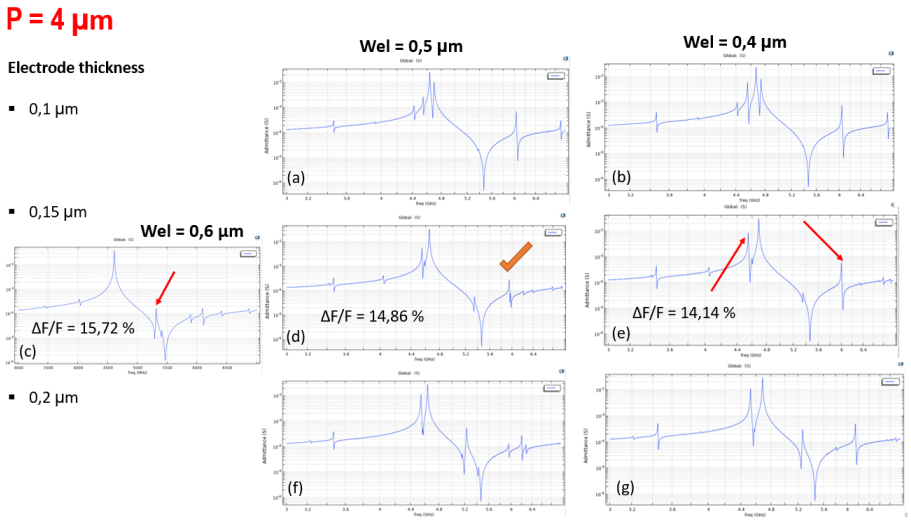

Figure 38: Admittance curves for different parameters combinations for $p = 4\mu m$

Modes identification

In order, to understand why contrary to the other pitch, there is no optimal parameters combinations, we will analyse the displacement field and stress tensor components of three main excited modes in different geometries, identified by a red arrow in figure 38.

The first excited mode following the anti-resonance is characteristic to lamb wave and it is $A13$ (figure 39). Its amplitude is lower for increasing width and thickness.

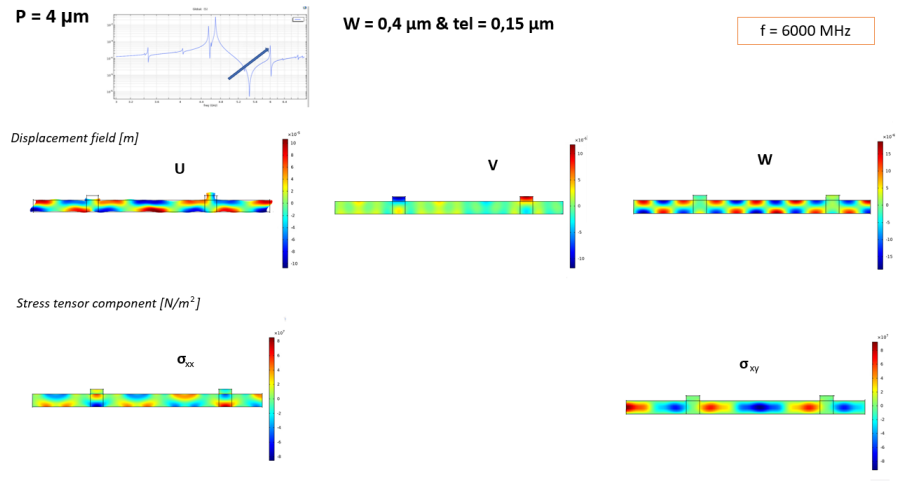

Figure 39: Displacement field and tensor stress to identify the spurious mode at f=6000Hz for $p = 4\mu m$, $w_{el} = 0.4\mu m$ and $t_{el} = 0.15\mu m$

In an other hand, the mode in the resonance pic (figure 44), which amplitude is more important for high electrode thickness and lower width, is non-trivial. We can identify a mixed of $A0$ and $A1$ modes which can be considered as an $SH0$ excitation.

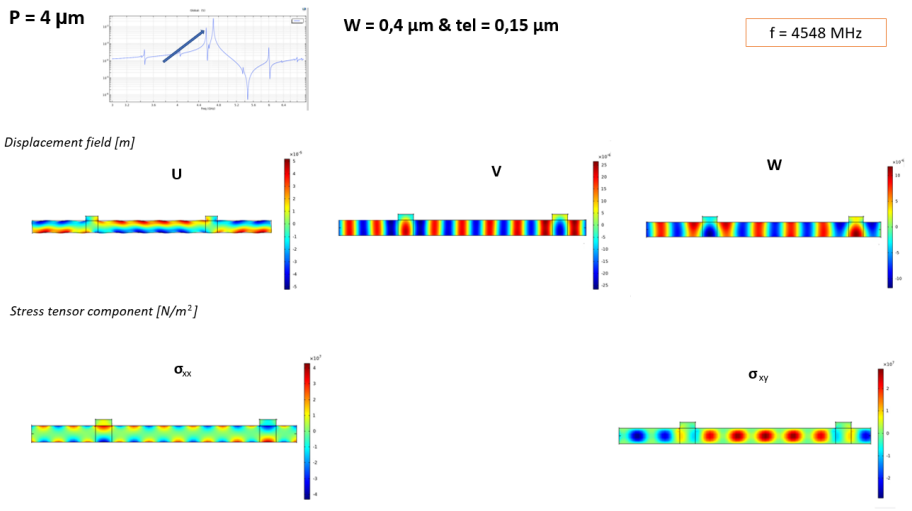

Figure 40: Displacement field and tensor stress to identify the spurious mode at f=4548Hz for $p = 4\mu m$, $w_{el} = 0.4\mu m$ and $t_{el} = 0.15\mu m$

The harmonic in the interval $f_s \leq f \leq f_p$ is also non-trivial and analysing the displacement and the stress does not allow to recognise any known mode (figure 41).

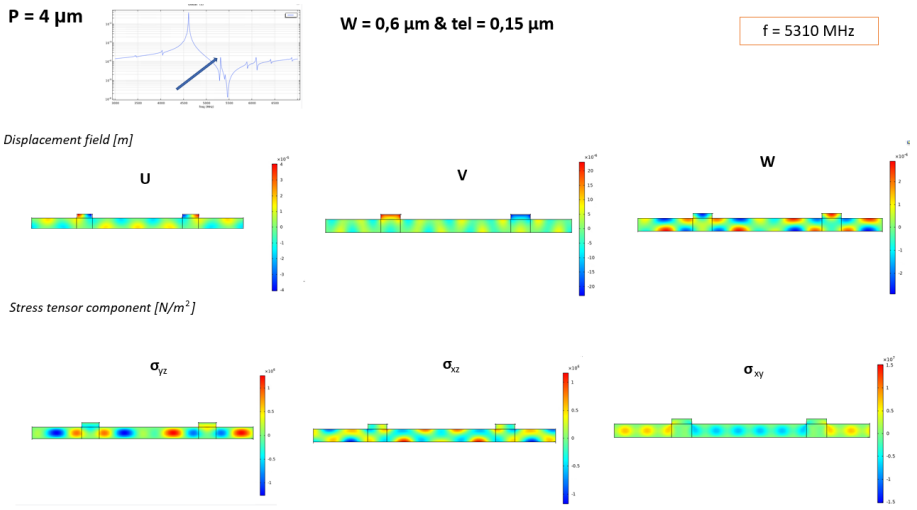

Figure 41: Displacement field and tensor stress to identify the spurious mode at f=5310Hz for $p = 4\mu m$, $w_{el} = 0.6\mu m$ and $t_{el} = 0.15\mu m$

Finally, as the identifications of the modes do not permit to clearly identify lamb waves modes, the behavior of the device for $p = 4\mu m$ is still not fully understood.

We can anyway retain that :

- the amplitude of lamb wave mode $A13$ decreases with higher width and thickness,
- the mode in between the resonance and anti-resonance $f_s \leq f \leq f_p$, as for $p = 3\mu m$ are non-trivial to identify,
- and finally, pics located closed to the resonance are symmetric.

Thickness proportionality $t_{pz} = t_{el}$

We will then see, if the thickness proportionality $t_{pz} = t_{el}$ gives better results.

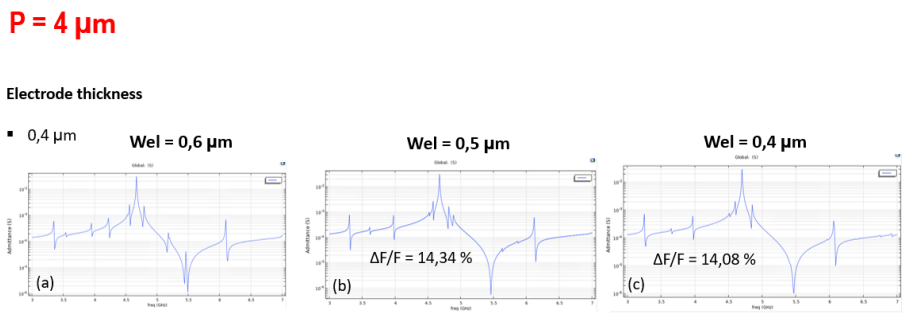

Figure 42: Admittance curves for $p = 4\mu m$, $t_{el} = 0.4\mu m$ and (a) $w_{el} = 0.6\mu m$, (b) $w_{el} = 0.5\mu m$, (c) $w_{el} = 0.4\mu m$

The results are still not convenient, always because of the excited mode close to the main pics.

However, if we have to choose combinations between all the one studied, '$w_{el} = 0.5\mu m$ and $w_{el} = 0.6\mu m$ with $t_{el} = 0.15\mu m$' and '$w_{el} = 0.4\mu m$ with $t_{el} = 0.4\mu m$' are equivalent in terms of admittance response. Only the electromechanical coupling change, and is higher for $w_{el} = 0.6\mu m$ with $t_{el} = 0.15\mu m$.

Finally, for $p = 4\mu m$ there is no particular optimal design.

Nevertheless, the following geometries can still be produced to be compared to the simulation.

- $w_{el} = 0.5\mu m$ with $t_{el} = 0.15\mu m$
- $w_{el} = 0.6\mu m$ with $t_{el} = 0.15\mu m$
- $w_{el} = 0.4\mu m$ with $t_{el} = 0.4\mu m$.

5.4.5 p = 5 μm

Parameters combinations

The results obtain for $p = 5\mu m$, figure 43 are appropriate for filters, especially for $t_{el} = 0.15\mu m$, (e) $w_{el} = 0.4$ and (d) $0.5\mu m$. There is only one harmonic, which is at a frequency higher than the anti-resonance and corresponds to a $A13$ mode represented in figure 44. *This mode is also observe for $p = 4\mu m$ also at a frequency higher than its anti-resonance at approximately the same location.* In the case of $p = 4\mu m$, the $A13$ mode present a decreasing amplitude for higher values of width and thickness.
It is also correct for $p = 5\mu m$ (as we can see in figure 43).

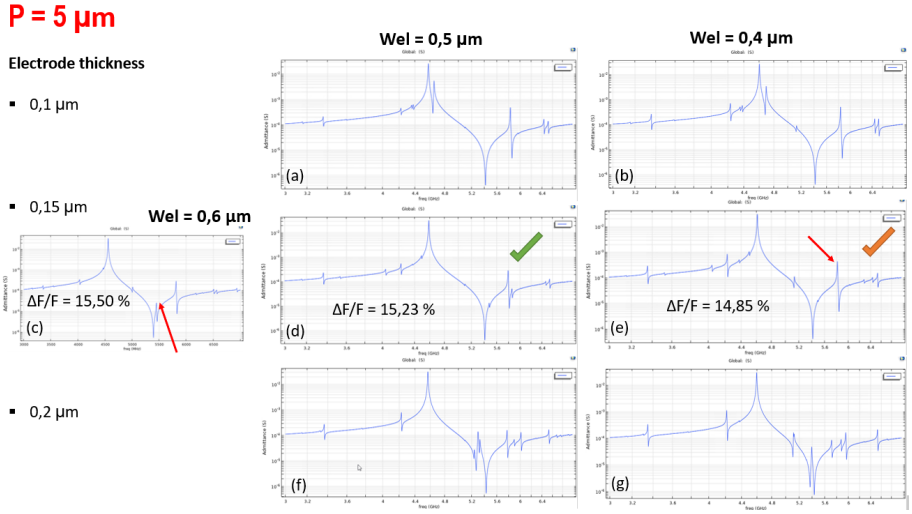

Figure 43: Admittance curves for different parameters combinations for $p = 5\mu m$

Modes identification

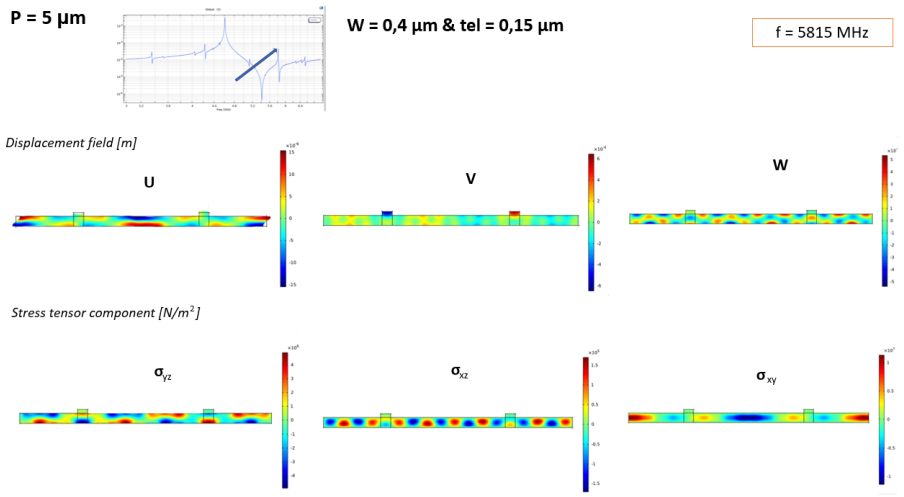

Figure 44: Displacement field and tensor stress to identify the spurious mode at f=5815Hz for $p = 5\mu m$, $w_{el} = 0.4\mu m$ and $t_{el} = 0.15\mu m$

The combination (c) $t_{el} = 0.15\mu m$ and $w_{el} = 0.6\mu m$ is also interesting as it has the biggest electromechanical coupling. Nevertheless, we identify an $S0$ mode (see figure 45) close to the anti-resonance which makes the resonator unusable.

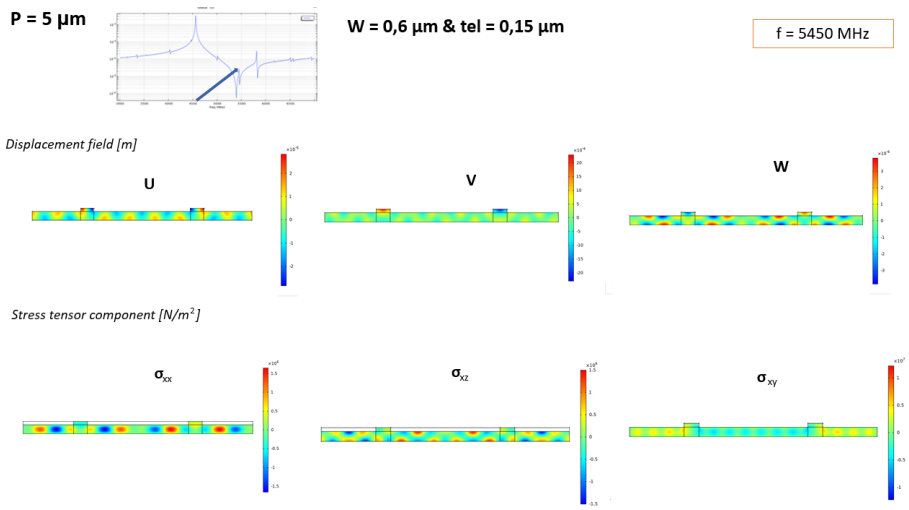

Figure 45: Displacement field and tensor stress to identify the spurious mode at f=5450Hz for $p = 5\mu m$, $w_{el} = 0.6\mu m$ and $t_{el} = 0.15\mu m$

The conclusion for $p = 5\mu m$ are similar to the one for $p = 4\mu m$:

- the amplitude of lamb wave mode $A13$ decreases with higher width and thickness,
- and pics located closed to the resonance are symmetric.

Thickness proportionality $t_{pz} = t_{el}$

The response of the filter is similar to the one obtain for $p = 4\mu m$ (when $t_{pz} = t_{el}$). The presence of small pics figure 46 decreases for $w_{el} = 0.4\mu m$. However, the thickness proportionality still do not give better results than $t_{el} = 0.15\mu m$. In addition, the electromechanical coupling is lower compared to the different combinations with $t_{el} = 0.15\mu m$.

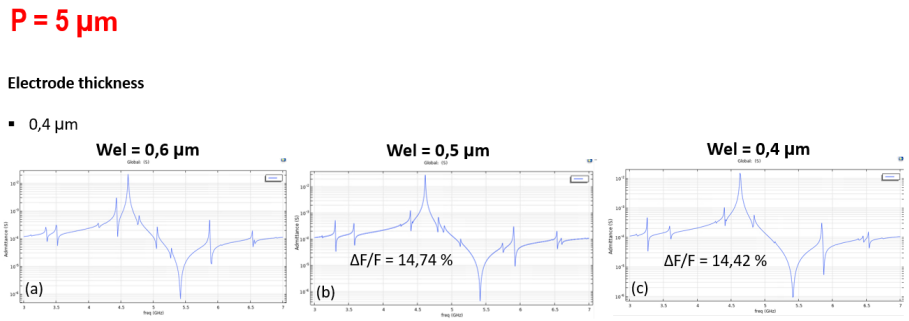

Figure 46: Admittance curves for $p = 5\mu m$, $t_{el} = 0.4\mu m$ and (a) $w_{el} = 0.6\mu m$, (b) $w_{el} = 0.5\mu m$, (c) $w_{el} = 0.4\mu m$

Finally, the optimal parameter combination for $p = 5\mu m$ is : $t_{el} = 0.15\mu m$ and $w_{el} = 0.5\mu m$.

The two combinations $p = 5\mu m$, $w_{el} = 0.4\mu m$, $t_{el} = 0.4$ and $0.15\mu m$ are still admissible and can be explored.

However, no parameters combination permit to suppress the $A13$ mode.

5.4.6 p = 6 μm

For $p = 5\mu m$, we have found optimal design which present a high electromechanical coupling with only one excited mode. We also notice that the behavior of the resonator is more stable for increasing pitch.

Parameters combinations

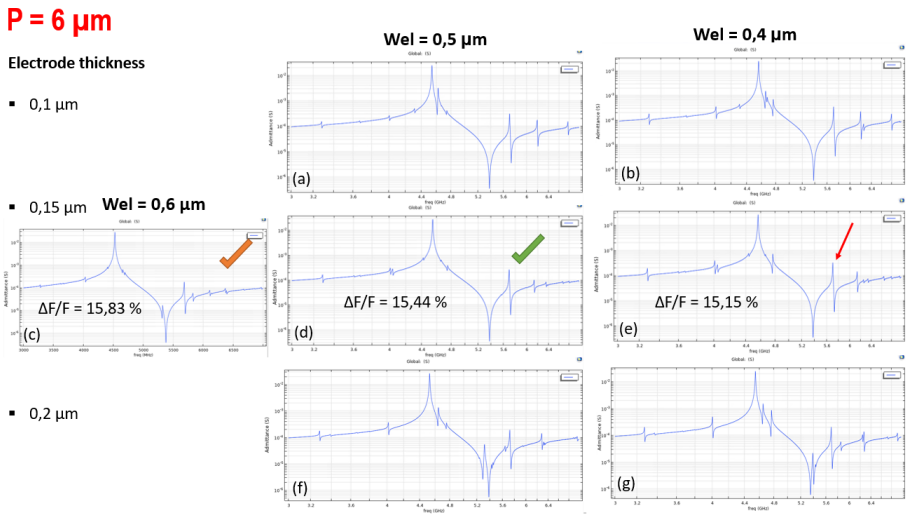

Figure 47: Admittance curves for different parameters combinations for $p = 6\mu m$

The admittance response for $p = 6\mu m$ follows the same trend as for $p = 5\mu m$. We can identify in figure 47, that $w_{el} = 0.6$ and $0.5\mu m$ for $t_{el} = 0.15\mu m$ are good combinations with only one main harmonic excited after f_p, as for $p = 4$ and $5\mu m$.

The difference between these two design is that for $w_{el} = 0.6\mu m$, there is a small pic next to the anti-resonance, with a negligible amplitude.

Modes identification

The harmonic just after the anti-resonance frequency also corresponds to the lamb wave mode $A13$ (see figure 48).

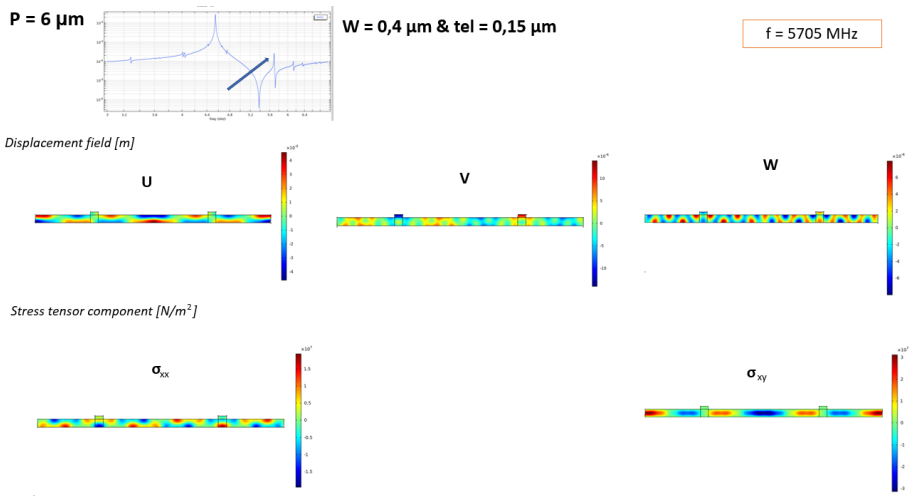

Figure 48: Displacement field and tensor stress to identify the spurious mode at f=5705Hz for $p = 6\mu m$, $w_{el} = 0.4\mu m$ and $t_{el} = 0.15\mu m$

The electromechanical coupling for $t_{el} = 0.15\mu m$, $w_{el} = 0.5\mu m$ and $w_{el} = 0.6\mu m$ are interesting and higher than for the other pitch. The only inconvenient of these designs is the fact that the mode $A13$ is close to the anti-resonance. Therefore, if we can find a way to eliminate it or to push it in higher frequencies, the resonator will surpass the others performances.

Evolution of $A13$ mode with width increments

First of all, the optimal electrode thickness in all cases is $0.15\mu m$. Therefore, the only geometrical parameter we can vary in order to study the evolution of the $A13$ mode is the electrode width w_{el}.

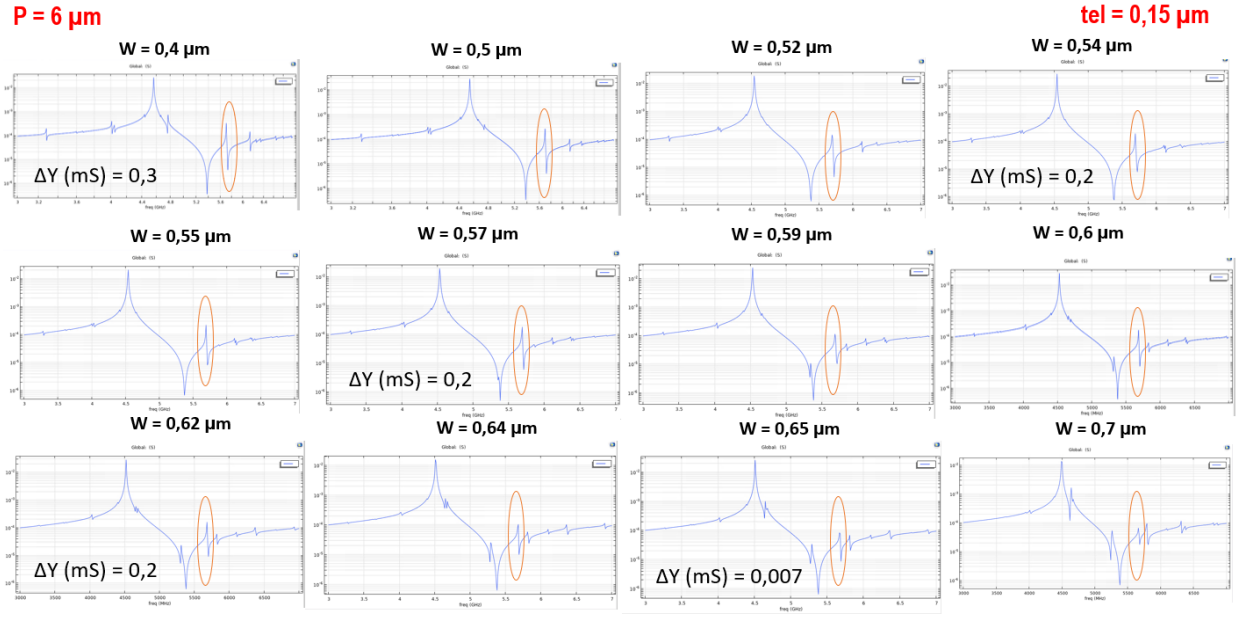

Figure 49: Evolution of $A13$ mode with width increments

If we increment the width as shown in figure 49, we can notice that the amplitude of the $A13$ mode (circled in orange) decreases with increasing width but never disappears. Its amplitude indeed become smaller, which is an interesting point, but at the same time, as we predicted new harmonics appears.

Finally, varying the width of the electrode only permits to decrease the amplitude of the lamb wave mode but its frequency does not change. *And increasing the width is not the best solution because it excites other modes.*

Thickness proportionality $t_{pz} = t_{el}$

For this pitch, the thickness proportionality gives exploitable but not optimal results for $w_{el} = 0.5\mu m$ and $w_{el} = 0.4\mu m$ (figure 50).

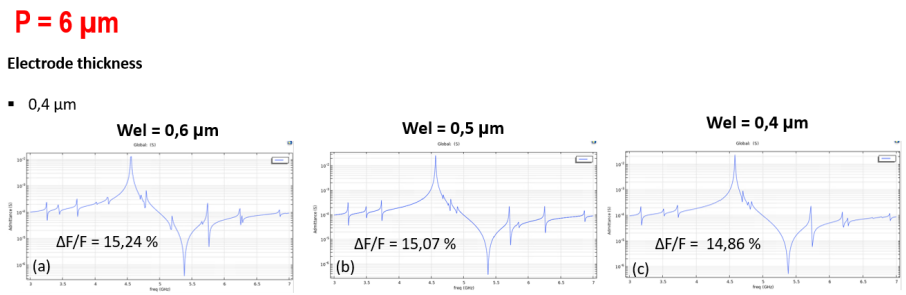

Figure 50: Admittance curves for $p = 6\mu m$, $t_{el} = 0.4\mu m$ and (a) $w_{el} = 0.6\mu m$, (b) $w_{el} = 0.5\mu m$, (c) $w_{el} = 0.4\mu m$

We can thus conclude that the optimal parameter combination for $p = 6\mu m$ is : $t_{el} = 0.15\mu m$ and $w_{el} = 0.5\mu m$.

The design $p = 6\mu m$ is : $t_{el} = 0.15\mu m$ and $w_{el} = 0.6\mu m$ can as well be produced.

As for $p = 5$ and $4\mu m$ no parameters combination permit to suppress the $A13$ mode.

5.4.7 p = 10 μm

Parameters combinations

Finally, for the last pitch, contrary to the order one, the appropriate width is higher and is equal to $0.6\mu m$.

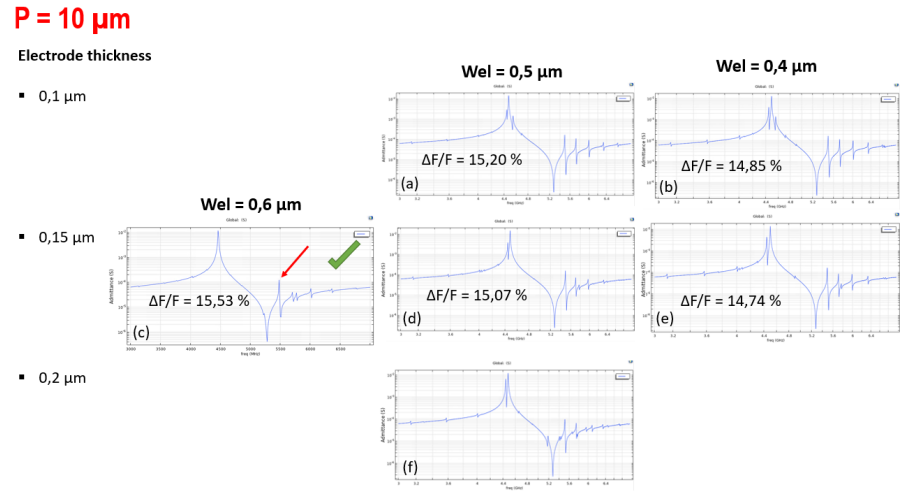

Figure 51: Admittance curves for different parameters combinations for $p = 10\mu m$

As we can see in the admittance-frequency curves in the figure 51, the other parameters combinations are not usable, because a mode near the resonance is excited, and with increasing thickness we can barely distinguish the harmonic from the main frequency. Fortunately, this mode disappears for $w_{el} = 0.6\mu m$.

Modes identification

Therefore for $w_{el} = 0.6\mu m$, there is only one unwanted mode after the anti-resonance frequency, as for $p \geq 4\mu m$. However, contrary to the other pitch values, the fact that the mode corresponds to $A13$ is not trivial. As we can see in the figure 53, the type of excitation seems to be an intermediate between $SH1$ and $A13$.

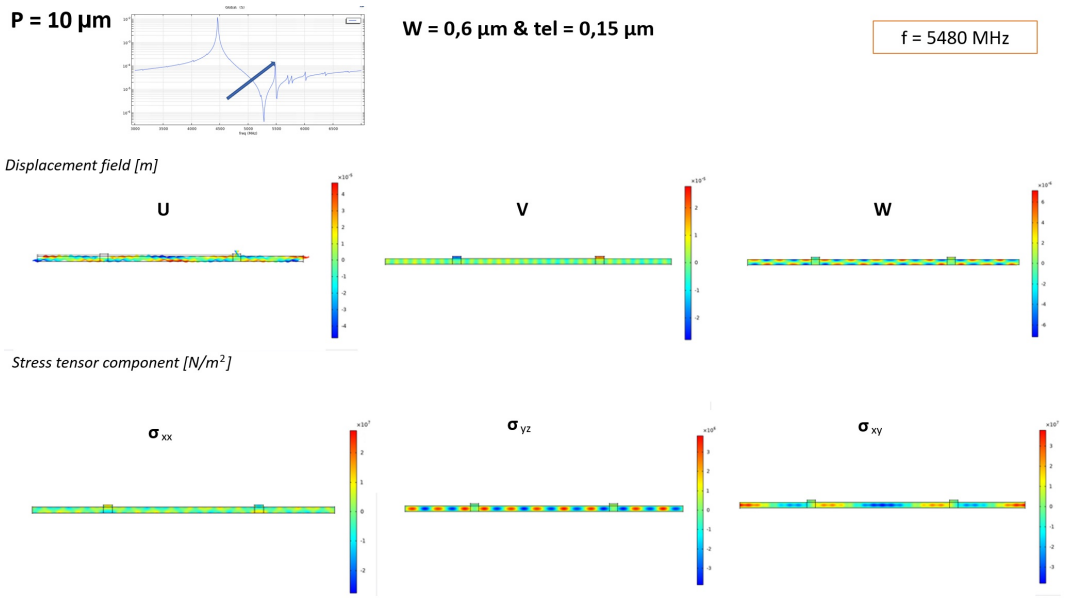

Figure 52: Displacement field and tensor stress to identify the spurious mode at f=5480Hz for $p = 10\mu m$, $w_{el} = 0.6\mu m$ and $t_{el} = 0.15\mu m$

Thickness proportionality $t_{pz} = t_{el}$

The thickness proportionality almost permits to suppress the mode close to the main pic and the behavior is similar to the one obtain for $w_{el} = 0.6\mu m$, with lower electromechanical coupling and higher amplitude mode after the $SH1$-$A13$ excitation.

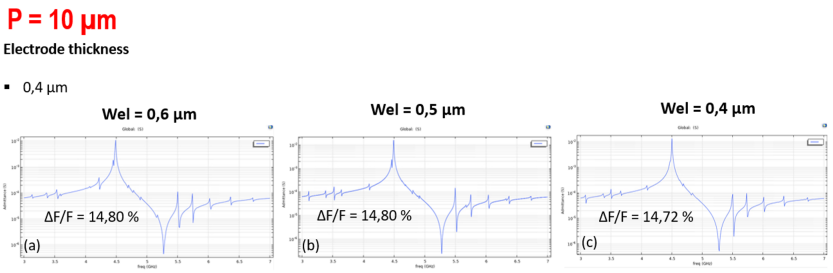

Figure 53: Admittance curves for $p = 10\mu m$, $t_{el} = 0.4\mu m$ and (a) $w_{el} = 0.6\mu m$, (b) $w_{el} = 0.5\mu m$, (c) $w_{el} = 0.4\mu m$

Therefore, the optimal parameter combination for $p = 10\mu m$ is : $t_{el} = 0.15\mu m$ and $w_{el} = 0.6\mu m$.

The design $p = 10\mu m$ is : $t_{el} = 0.4\mu m$ can as well be produced.

Finally, analysing all the data, lead us to the conclusion that more we increase the pitch, less the response of the resonator becomes sensible to geometrical parameters variations.

6 Conclusion

The different geometrical parameters, *pitch electrode width and thickness* have an influence on the behavior of the resonator. Increasing the width and thickness mainly impact the stability of the device (important number of excited modes). Their influence is more important for smaller pitch whereas, bigger one are less sensible to design changes.

The challenge is thus to find geometries that have a good compromise between the number of harmonics, their location and the electromechanical coupling. Identifying the excited modes permit to have a better understanding of the admittance response of XBAR resonators. We have seen that for $p \geq 4\mu m$, the first harmonic at a frequency higher than the anti-resonance is the horizontal $A13$ lamb wave mode. It presence and amplitude depend on the electrode width and thickness. Increasing these parameters, tend to vanish this mode. But it is still not the solution, as new ones are excited.
However, the harmonics does not always corresponds to a known excitation type, especially when their frequency is in between the resonance and anti-resonance : $f_s \leq f \leq f_p$.

The thickness equality between the piezoelectric membrane and the metallic electrode didn't give convenient results for all pitch. The response of the device is only acceptable for $p \geq 4\mu m$ and specific electrode width. Therefore, we can generally say that bigger pitch are more interesting in terms of stability and electromechanical coupling.

Finally, XBAR resonator have a high resonance frequency, approximately around 4-5GHz, which also depend on the geometrical parameters and especially on the pitch and electrode width. The electromechanical coupling is also important, and we achieve more than 15% for optimal designs.

Optimal design in order of performance

1. $p = 10\mu m$ - $t_{el} = 0.15\mu m$ - $w_{el} = 0.6\mu m$
2. $p = 6\mu m$ - $t_{el} = 0.15\mu m$ - $w_{el} = 0.5\mu m$
3. $p = 5\mu m$ - $t_{el} = 0.15\mu m$ - $w_{el} = 0.5\mu m$
4. $p = 2\mu m$ - $t_{el} = 0.15\mu m$ - $w_{el} = 0.5\mu m$
5. $p = 3\mu m$ - $t_{el} = 0.15\mu m$ - $w_{el} = 0.5\mu m$

References

[BCS+04] Gang Bu, D. Ciplys, Michael Shur, L. Schowalter, Sandra Schujman, and Remis Gaska. Electromechanical coupling coefficient for surface acoustic waves in single-crystal bulk aluminum nitride. *Applied Physics Letters*, 84:4611 – 4613, 07 2004.

[GP13a] Songbin Gong and Gianluca Piazza. Design and analysis of lithium-niobate-based high electromechanical coupling rf-mems resonators for wideband filtering. *IEEE Transactions on Microwave Theory Techniques*, 61:403–414, 01 2013.

[GP13b] Songbin Gong and Gianluca Piazza. Design and analysis of lithium-niobate-based high electromechanical coupling rf-mems resonators for wideband filtering. *IEEE Transactions on Microwave Theory Techniques*, 61:403–414, 01 2013.

[HB] Gianluca Piazza Harmeet Bhugra. *Piezoelectric MEMS Resonators*, volume Microsyst., Nanosystems. Springer, Cham.

[LYLG20] Ruochen Lu, Yansong Yang, Steffen Link, and Songbin Gong. A1 resonators in 128° y-cut lithium niobate with electromechanical coupling of 46.4 *Journal of Microelectromechanical Systems*, PP:1–7, 04 2020.

[SDL+18] Xiaoqiang Sun, Xiangyan Ding, Feilong Li, Shijie Zhou, Yaolu Liu, Ning Hu, Zhongqing Su, Youxuan Zhao, Jun Zhang, and Mingxi Deng. Interaction of lamb wave modes with weak material nonlinearity: Generation of symmetric zero-frequency mode. *Sensors*, 18:2451, 07 2018.

[SYZ+20] Hao Shi, Liang Yan, Yuanzhen Zheng, Tingfeng Ma, Mingfei Wang, Bin Huang, Lili Yuan, Ji Wang, Jianke Du, and Han Zhang. Piezoelectric resonators excited by lateral electric fields based on a litao3 single crystal. *Crystals*, 10:525, 06 2020.

[Wei85] Gaylord T.K. Weis, R.S. Lithium niobate: Summary of physical properties and crystal structure. *IEEE Transactions on Ultrasonics Ferroelectrics and Frequency Control*, Appl. Phys. A 37, 191–203, 1985.

[YPK+19] Soumya Yandrapalli, Victor Plessky, Julius Koskela, Ventsislav Yantchev, Patrick Turner, Guillermo Luis, and Villanueva. Analysis of xbar resonance and higher order spurious modes. 11 2019.

[YXF+07] Jiashi Yang, Huan Xue, Huiyu Fang, Yuantai Hu, Ji Wang, and Lijun Shen. Effects of electrodes with varying thickness on energy trapping in thickness-shear quartz resonators. *IEEE Transactions on Ultrasonics Ferroelectrics and Frequency Control*, 54, 05 2007.

[ZL16] Jie Zou and Chern Shi Lam. Electrode design of aln lamb wave resonators. pages 1–5, 05 2016.

[Zou15] J Zou. High-performance aluminum nitride lamb wave resonators for rf front-end technology. uc berkeley. 2015.

List of Figures

List of Tables